

University of Southern Queensland

School of Engineering

**Dynamic Assessment of System Inertia in Emerging
Transmission Networks in Real Time**

A dissertation submitted by

Brad Christopher

in fulfillment of the requirements of

ENP4111 Professional Engineer Research Project

towards the degree of

Bachelor of Engineering Honours

2024

This page intentionally left blank

University of Southern Queensland

School of Engineering

ENP4111 Dissertation Project

(This is a 2-unit research project in Bachelor of Engineering Honours Program)

Limitations of Use

The Council of the University of Southern Queensland, its Academic Affairs, and the staff of the University of Southern Queensland, do not accept any responsibility for the truth, accuracy or completeness of material contained within or associated with this dissertation.

Persons using all or any part of this material do so at their own risk, and not at the risk of the Council of the University of Southern Queensland, its Faculty of Health, Engineering and Science or the staff of the University of Southern Queensland.

This dissertation reports an educational exercise and has no purpose or validity beyond this exercise. The sole purpose of this dissertation project is to contribute to the overall education within the student's chosen degree program. This document, the associated hardware, software, drawings, and other material set out in the associated appendices should not be used for any other purpose: if they are so used, it is entirely at the risk of the user.

CERTIFICATION

I certify that the ideas, designs and experimental work, results, analyses, and conclusions set out in this dissertation are entirely my own effort, except where otherwise indicated and acknowledged.

I further certify that the work is original and has not been previously submitted for assessment in any other course or institution, except where specifically stated.

Student Name Brad Christopher

Student Number:



Signature

____4th November 2024____

Date

ABSTRACT

Burning fossil fuels for power generation is one of the highest sources of pollution around the world. Governments have committed to carbon reduction targets to reduce the rate of environmental damage occurring. To achieve these goals low or zero carbon emitting renewable energy resources are being installed on networks which displace legacy synchronous generation.

Historically the power system has had a high level of power system inertia as the network contains multiple synchronous generators in lock step with other, maintaining the power frequency, providing system stability, and keeping the balance between power generated and load power. An unknown variable is what the impact of renewable resources will have on the system inertia as, due to their design, they provide little to no inertial response to system disturbances.

This project aimed to develop a method for transmission network system operators to assess system inertia in real time. Different methods of achieving this were examined. The final product of the research lead to the development of a sliding discrete Fourier transform that monitors the voltage waveform. This can be simply implemented on existing network infrastructure and works independently without requiring any load or generation information.

ACKNOWLEDGEMENTS

First, I would like to thank Dr Yi Cui for his assistance and guidance through the course of developing this dissertation.

Second, I would like to thank my family for their unwavering supporting and encouragement through the various demands of, not only this dissertation, but the course in its entirety.

Also, I would like to thank my work colleagues for their support.

TABLE OF CONTENTS

	PAGE
CERTIFICATION	iv
ABSTRACT	v
ACKNOWLEDGEMENTS	vi
TABLE OF CONTENTS	vii
LIST OF TABLES	xii
LIST OF FIGURES	xiii
NOMENCLATURE	xv
GLOSSARY	xvi
UNITS OF MEASURE	xvii
Chapter 1 INTRODUCTION	1
1.1 Aim – Context and importance.....	1
1.2 Background.....	1
1.3 Problem.....	3
1.4 Objectives	4
1.4.1 Objective 1: Research.....	4
1.4.2 Objective 2: Model Development	4
1.4.3 Objective 3: Data Collection	5
1.4.4 Objective 4: Inertia Tool Development	5
1.4.5 Objective 5: Actual Data Inertia Test	5

1.4.6 Outcomes and Benefits	5
Chapter 2 BACKGROUND & LITERATURE REVIEW	6
2.1 Synchronous Generation and Inertia	6
2.1.1 Synchronous Machines	6
2.1.2 Swing Equation	7
2.2 System Stability and Inertia.....	13
2.2.1 Generator Power Angle and Capability Curve	14
2.2.2 Inertia and Acceleration.....	14
2.2.3 Inertia and Deceleration.....	15
2.2.4 Low System Inertia.....	15
2.3 Disturbances	16
2.4 Operating Standards	16
2.5 Frequency	17
2.6 New Generation.....	19
2.6.1 Renewable Energy Sources	19
2.6.2 Battery Energy Storage Systems	19
2.7 Inverter Based Resources	20
2.7.1 Grid Following Inverters	20
2.7.2 Grid Forming Inverters.....	21
2.7.3 IBR and Inertia	21
2.7.4 Location Concerns	23

2.8 Rate of Change of Frequency (RoCoF)	23
2.8.1 RoCoF Performance	25
2.9 SCADA.....	27
2.10 Chapter Summary	29
Chapter 3 METHODOLOGY	30
3.1 Simulink model	30
3.1.1 Model Components	31
3.1.1.2 Generators.....	31
3.1.1.3 Automatic Voltage Regulator.....	32
3.1.1.4 Prime Mover and Governor.....	32
3.1.1.5 AVR and Exciter Block.....	33
3.1.1.6 Prime Mover and Governor Block	34
3.1.1.7 Network Components	37
3.2 Measurement of RoCoF	37
3.2.1 Zero Crossing	37
3.2.1.1 Piecewise	38
3.2.1.2 Least Squares.....	39
3.2.1.3 Input Filtration.....	39
3.2.2 Discrete Fourier Transform	39
3.2.3 FFT	40
3.2.4 Three Level DFT	42

3.2.5 Sliding DFT	43
3.3 RoCoF.....	43
3.4 Nyquist Frequency.....	44
3.5 Chapter Summary	44
Chapter 4 RESULTS AND DISCUSSIONS.....	45
4.1 Simulink Network Model	45
4.1.1 Model Tests	47
4.1.1.1 Test 1. Small Disturbance.....	48
4.1.1.2 Test 2. Droop Adjustment	49
4.1.1.3 Test 3. Large Disturbance.....	50
4.1.1.4 Test 4. Large Disturbance and Loss of Generator	51
4.1.1.5 Test 5. Salient Pole Synchronous Generator	52
4.1.1.6 Test 6. One Synchronous Generator.....	53
4.1.2 Summary of Simulink Results.....	54
4.2 Frequency Assessment	55
4.2.1 Overview	55
4.2.2 Generator Settings	55
4.2.3 Zero Crossing	56
4.2.4. DFT.....	59
4.2.4.1 Sampling Frequency	59
4.2.4.2 Peaks.....	61

4.2.4.3 Results of DFT	61
4.2.4.4 DFT Accuracy	62
4.2.4.5 Results of Zero Padding	63
4.2.5 RoCoF.....	66
4.2.6 Sliding DFT	67
4.2.7 Chapter Summary	70
Chapter 5 CONCLUSIONS	71
FURTHER WORK.....	72
Chapter 6 Reference list	73
APPENDIX A Specification	76
APPENDIX B Model Overview	81
APPENDIX C MATLAB CODE.....	90

LIST OF TABLES

Table 1 Typical inertia constant values	12
Table 2 AEMC Frequency operating standard definition of credible and non-credible	17
Table 3 AEMC Frequency operating bands	18
Table 4 AEMC Frequency operating standard for RoCoF.....	26
Table 5 Tests completed using Simulink model.....	47
Table 6 Calculated RoCoF performance	54
Table 7 Results of zero crossing sample.....	58
Table 8 Initial DFT results.....	61
Table 9 Fundamental frequency comparison.....	63

LIST OF FIGURES

Figure 2.1 Frequency response to a system disturbance (WU et al.,2017)	13
Figure 2.2. Generator power angle, (Babu, .2022)	15
Figure 3.1 Simulink model (based on Mathworks Model).....	31
Figure 3.9 Orthogonal decomposition of a waveform (Seeber & Ulrici. 2016).	41
Figure 4.11. Test 1 small disturbance	48
Figure 4.12. Test 2 demonstration of droop setting change.....	49
Figure 4.13. Test 3 Large disturbance test.....	50
Figure 4.14. Test 4 Large disturbance and loss of generation	51
Figure 4.15 Test 5 Salient pole generators	52
Figure 4.16 Test 6 simulation of a lack of inertia.....	53
Figure 4.17 Test 3 data for RoCoF	54
Figure 4.18 Test 6 data for RoCoF	54
Figure 4.19 Example code in MATLAB for model settings	56
Figure 4.20. Example of adjusting settings via command window	56
Figure 4.21. Zero crossing error - multiple zero crossings due to harmonic content	57
Figure 4.22 DFT process display – 50 Hz fundamental	64
Figure 4.23. DFT process display - 51.11 Hz fundamental	65

Figure 4.24 South Australia state outage	66
Figure 4.25 Reproduced frequency profile for SA event (last 1.8 seconds only).....	67
Figure 4.26. Result of SDFT versus sample frequency	69
Figure 4.27 Example system operator RoCoF alert.....	69

NOMENCLATURE

J	Moment of inertia of a rotating mass
θ_m	Angular displacement of a rotor with respect to a stationary axis
T	Torque
T_m	Mechanical torque
T_e	Electrical torque
T_a	Accelerating torque
ω	Angular velocity
ω_{sm}	Synchronous speed
δ_m	angular displacement of the rotor in mechanical radians
δ	Load angle
P_a	Accelerating power
P_e	Electrical power
P_m	Mechanical power
K_e	Kinetic energy

GLOSSARY

Abbreviations

AC	Alternating Current
DC	Direct Current
AEMC	Australian Energy Market Commission
AEMO	Australian Energy Market Operator
DFT	Discrete Fourier Transform
FCAS	Frequency control ancillary support
IBR	Inverter Based Resource
NEM	National Electricity Market
NER	National Electricity Rules
PV	Photovoltaic
TNSP	Transmission Service Provider
RES	Renewable Energy Resource
GFL	Grid Following Inverter
GFM	Grid Forming Inverter

UNITS OF MEASURE

V Voltage – potential difference between two points

W Watt – unit of power. 1 Watt = 1 joule per second

VA Volt – Amperes - Reactive power



CHAPTER 1 INTRODUCTION

1.1 AIM – CONTEXT AND IMPORTANCE

The objective of this research is to develop a real-time power system inertia estimation tool that give Transmission and Network Providers (TNSPs) the ability to gauge their system security. In context of a power system, security refers to the rate at which key technical parameters might change and the ability of the system to withstand disturbances.

Power system inertia is the aggregate equivalent inertia of all devices on the power system capable of providing inertial response, which is the initial, instantaneous electrical power transfer from an apparatus in response to a disturbance in the power network. The disturbance, a large event that ripples through the network, affects the balance between generated power and load power and is readily recognisable by its impact on the power system frequency.

As the power balance must be maintained, the system frequency must be strictly controlled within rigid constraints to avoid loss of both generation and loads and as such is a key part of system security.

The outcome of the project will be a method which can utilise existing parameters to determine the system inertia which can be overlaid on a network diagram, so any problematic areas are rapidly recognisable.

1.2 BACKGROUND

Traditional power networks are made up of a combination of synchronous generators connected in parallel to form a network. The combination of many synchronous generators



gives the system strength as each generator is held in lock step with the majority. Each synchronous generator used for power generation is a large heavy machine that contains a heavy spinning rotor. The kinetic mass of this rotor has substantial mechanical inertia, which is electro-magnetically coupled to the power network and thus provides power system inertia.

The speed of the rotor in the generator is governed to within strict limits. The reason for such tight control is that the speed of the generator establishes the power frequency on the network, the level of which is critical to the function of the power network and connected loads. If the frequency drifts too high or low it can have a rapid and detrimental impact on connected loads, sensitive equipment and most importantly the security and stability of the network. Automatic protection schemes are installed at all levels of a power system from high voltage generation through transmission, sub-transmission, distribution, and low voltage that will disconnect/ trip during a frequency related disturbance. Losing large loads or generators during a disturbance can cause a cascading effect that sees further load disconnection via schemes such as under frequency load shedding.

A power network with a satisfactory level of system inertia will ride through most disturbances and will not allow the frequency to exceed limits easily. This is because the aggregate total of the network generators' own inertia resists the electromagnetic force of a disturbance, thereby maintaining network frequency. Good levels of system inertia ensure the effects of any disturbance are localised to the site of the disturbance, thereby minimising the volume of affected consumers or industry.



1.3 PROBLEM

The process of generation of electricity on a mass scale and the industrialisation and urbanisation of our way of life has resulted in severe degradation of our natural environment. A major cause of this pollution is the release of Carbon Dioxide into the atmosphere, with the most substantial contribution of CO₂ coming from the energy sector. As a consequence, governments and authorities around the world have developed strategies to reduce emissions.

As part of the emission reduction strategy there has been a push to increase the number of large-scale renewable energy sources (RES) connecting to power networks. This has seen a reduction in the number of synchronous generators supplying networks as they are displaced by the renewable energy resource or inverter-based resources (IBR).

Inverter based resources use electronic converter technology to connect the generation source to the power network. The disadvantage of this design is even if the generation may involve some sort of inertia i.e., a wind turbine, it is not possible for that inertia to be electromagnetically coupled to the power network, as it was with a synchronous generation, due to the power electronics conversion associated with the IBR. The increasing connection of these inverter-based technologies has negatively impacted the traditional power system inertia.

The full impact of the reduction of power system inertia is not clearly available to network operators, as any shortfall only becomes apparent during a large network disturbance. Manufacturers of the renewable energy resources technology are aware of this problem and a considerable amount of work has been completed on creating virtual or synthetic inertia

from renewable energy resources. This virtual inertia is modelled on the characteristics of a synchronous generator to allow it to mimic it during a network disturbance or upon initial energisation.

There remains questions and concerns about the ability of virtual inertia to perform to an equivalent level of a synchronous generator during a system disturbance. Indications are power networks will have to maintain around 20% of the connected synchronous generators for system stability. Renewable energy resources characteristics are modelled on synchronous generators and rely on their inertial stability for a reference when connected to the power system, further there are concerns as to how they would perform when a substantial network disturbance occurs.

1.4 OBJECTIVES

The overall aim of this dissertation is to provide a detailed study of the impact of renewable energy source connections to the power system inertia and to provide a method of dynamic real time measurement of that inertia. The following six points establish the main objectives for the research,

1.4.1 Objective 1: Research

Provide relevant evidence that RES impacts power system inertia. Devise a practical solution to address the theoretical problem.

1.4.2 Objective 2: Model Development

Using industry accepted programs produce a suitable network model that realistically mimics an actual network upon which simulations of disturbances can occur, to gauge the impact of the system frequency.



1.4.3 Objective 3: Data Collection

Obtain real data from a known event to test network model

1.4.4 Objective 4: Inertia Tool Development

Develop a tool that can display the system inertia in real time

1.4.5 Objective 5: Actual Data Inertia Test

Obtain actual data or use simulated event to test the model and inertia tool

1.4.6 Outcomes and Benefits

The outcomes expected of this proposal are:

- An improved understanding of system inertia for TNSPs in general and network operators
- Improved visibility of the state of the power system inertia in real time
- TNSPs will be better equipped to respond to network disturbances and could respond to potential network security shortfalls before they cause outages

The benefits of this project are expected to be:

- Improved network security. Less of the network is at risk of unplanned outages due to lack of inertia
- Improved network stability. Network operators and planners have better oversight of the network
- Consumers will experience less nuisance outages



CHAPTER 2 BACKGROUND & LITERATURE REVIEW

2.1 SYNCHRONOUS GENERATION AND INERTIA

System inertia is not an inherent power system requirement, rather, it is a characteristic of synchronous machines which has the benefit of providing a fundamental stabilising effect on the power system frequency. Both AEMO (2020) and Denholm et al. (2020) acknowledge the traditional formation of a power system using synchronous generation, stating the networks are connected to many large synchronous generators synchronised together i.e., in lock step. Power system inertia is the aggregate equivalent inertia of all devices on the power system capable of providing an internal response (AEMO).

2.1.1 Synchronous Machines

Power system inertia is linked to the mechanical inertia of the synchronous generator, via electro-mechanical coupling. The synchronous generator is a synchronous machine that is also able to be a motor. The two principal parts of the machine are both ferromagnetic structures. The stationary part, or stator, is a long hollow cylinder that contains longitudinal slots for armature windings. The armature windings carry current to the network. The other principal part is the rotor, which is mounted on a shaft and rotates inside the machine. The winding on the rotor is referred to as the field winding and this is supplied with a direct current (DC). The shaft of the synchronous generator is driven by a prime mover, traditionally in large generation plants a steam turbine (Grainger and Stevenson, 1994). In a large generator a lot of mechanical inertia is created due to the large ferromagnetic construction with an equally large turbine rotating the generator.



2.1.2 Swing Equation

Grainger and Stevenson (1994) establish the swing equation is a fundamental equation that governs the rotational dynamics of a synchronous machine and includes the impact of the machines' mechanical inertia. By deriving the swing equation, the direct relationship between the mechanical inertia and the electrical inertia becomes apparent. The equation links the power input from the prime mover to the power output onto the network and demonstrates how the rotor inertia responds to disturbances on the power system. Essentially the prime mover of a generator applies a torque to the rotor and the electrical load applies a counter torque to the rotor, when these two are equal the system is considered balanced, and the power network is stable.

For a synchronous generator the product of the moment of inertia of the rotor, the ratio between the torque applied and the resulting angular acceleration, multiplied by its angular acceleration yields the rotor motion of a synchronous machine.

For a synchronous generator, the equation is:

$$J \frac{d^2 \theta_m}{dt^2} = Ta = Tm - Te \quad (2.1)$$

Where,

J - Moment of inertia of the rotating mass (kgm²)

θ_m – angular displacement of the rotor with respect to a stationary axis

t – time in seconds

Tm – mechanical torque minus the retarding torque due to rotational losses

Te – the net electrical torque

Ta - the net accelerating torque

Referring to equation (2.1) the mechanical torque Tm and the electrical torque Te are positive values which implies that under a steady state condition the accelerating torque Ta is equal to zero. In this case there is an absence of accelerating or decelerating torque acting on the rotor and the machine would be at synchronous speed.

At steady state all synchronous generators in a power system are in synchronism, that is their rotors and turbines are all moving at synchronous speed. In (2.1) Te refers to the net losses across the air gap in the machine plus the I^2r losses, generally heating, in the armature winding.

θ_m is measured with respect to a stationary axis so is constantly increasing when the machine is operating i.e., constantly increasing. The main point of interest of a synchronous



machine is the rotor speed relative to the synchronous speed so an angle δm is measured, which is the difference between the rotor angular position with respect to a reference axis (rotating at synchronous speed). θm can now be expressed as:

$$\theta m = \omega_{sm} + \delta m \quad (2.2)$$

Where,

ω_{sm} - synchronous speed (rad/s)

δm - angular displacement of the rotor in mechanical radians (from the synchronously rotating reference axis)

The derivatives with respect to the time of (2.2) are

$$\frac{d\theta m}{dt} = \omega_{sm} + \frac{d\delta m}{dt} \quad (2.3)$$

and

$$\frac{d^2\theta m}{dt^2} = \frac{d^2\delta m}{dt^2} \quad (2.4)$$

When the $d\delta m$, change in angular displacement, value is zero the rotor angular velocity is constant and equals the synchronous speed (2.3). This indicates that the $d\theta m$ is the deviation in rotor speed from the synchronous speed in mechanical radians per second. As we now are using a rotating reference instead of a fixed reference (2.1) can now be adjusted to incorporate the rotating angular displacement δm as derived in (2.4).



$$J \frac{d^2 \delta m}{dt^2} = T a = T m - T e \quad (2.5)$$

The angular velocity of the rotor can be expressed by the term ω_m :

$$\omega_m = \frac{d\theta m}{dt} \quad (2.6)$$

So, taking into consideration the angular velocity of the rotor, the moment of inertia and the rotor acceleration, the accelerating power of the machine is

$$J \omega_m \frac{d^2 \delta m}{dt^2} = P a = P m - P e \quad (2.7)$$

Where,

$P a$ – accelerating power. This accounts for any unbalance between mechanical power input and the power generated by the loaded machine

$P m$ – mechanical power – prime mover

$P e$ – electrical power – electrical power output

(2.7) now introduces power in instead of torque, as power is equal to the torque multiplied by the angular velocity, hence the term $J \omega_m$. At synchronous speed the $J \omega_m$ term is called the inertia constant of the machine and is denoted by M . M is constant at synchronous speed and is a per-unit value.



Synchronous machine ratings can be supplied with a different constant which refers to inertia being the H constant, which is typically measured in seconds. This is defined by

$$H = \frac{\text{stored kinetic energy in Mj at synchronous speed}}{\text{machine rating in MVA}}$$

In physics kinetic energy equates the mass of the object and the square of its velocity:

$$Ke = \frac{1}{2} m v^2 \quad (2.8)$$

So, for H

$$H = \frac{\frac{1}{2} M \omega_{sm}}{S_{machine}} \text{ MJ/MVA} \quad (2.9)$$

Where,

$S_{machine}$ - three phase rating of the machine (MVA)

The inertia constant H denotes how long the generator rated output will be sustained by the inertia of the generator with no input from the prime mover.

Manipulating (2.9) to have it in respect to M and substituting this into (2.7) the resulting equation becomes

$$\frac{2H}{\omega_{sm}} \frac{d^2 \delta_m}{dt^2} = \frac{Pa}{S_{Machine}} = \frac{Pm}{S_{Machine}} - \frac{Pe}{S_{Machine}} W \quad (2.10)$$

Writing this in per unit form:

$$\frac{2H}{\omega_s} \frac{d^2 \delta}{dt^2} = Pa = Pm - Pe \text{ p.u.} \quad (2.11)$$

(2.11) is called the swing equation.

According to Chown et al. (2017), typical values for H are in the ranges as found in Table

1. These vary due to the moment of inertia, generator speed and unit size.

Table 1 Typical inertia constant values

Inertia Constant range (MWs/MVA)	Prime Mover type	rpm
2.5 – 6	Thermal	3000
4 - 10	Thermal	3000
2 - 4	Hydro	1500

2.2 SYSTEM STABILITY AND INERTIA

Inertia of the machine is a key factor in the performance of a synchronous generator (Grainger and Stevenson, 1994). The inertia constant of the machine H defines the ability of the machine to resist change in the angular rotation of its rotor. This provides system stability during sudden changes in load or sudden disconnection of generation; the rotor delivers its inertia to the system which dampens any system oscillation because of the disturbance. Figure 2.1 is an example of the frequency response to a system disturbance (WU et al., 2017), the inertial response can be observed from the instant the disturbance occurs to approximately half a second later. The inertia of the machine is released during this period as an opposing force to this change.

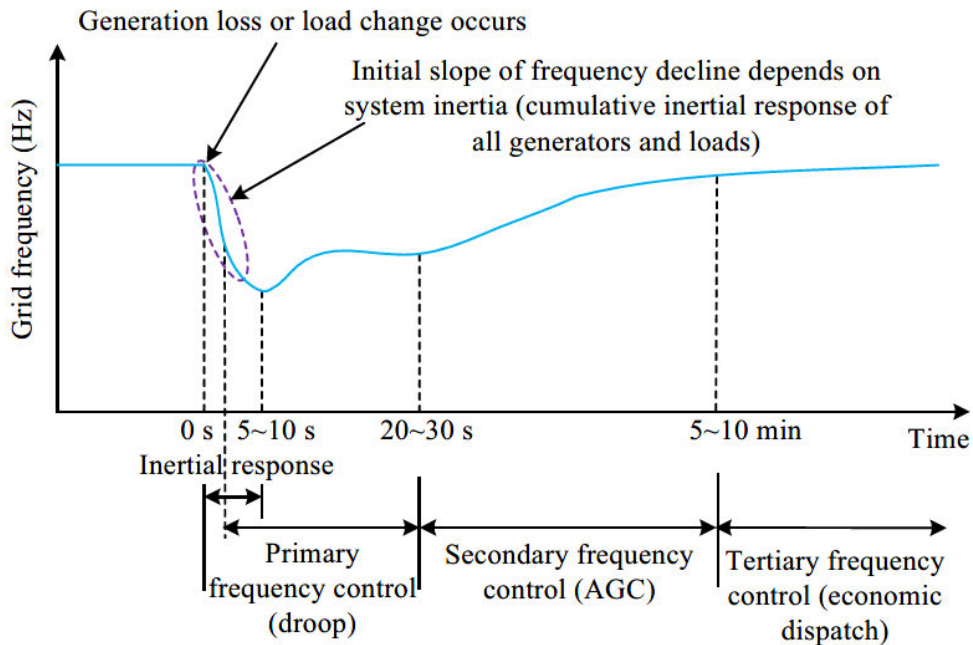


Figure 2.1 Frequency response to a system disturbance (WU et al., 2017)



Synchronous Generators have extensive external control systems for managing the speed of a prime mover, in figure 2.1 these activate from approximately half a second after the disturbance. These systems operate once the speed of the machine changes and therefore are outside the scope of this paper, as the inertial response has already been expelled when the speed changes.

2.2.1 Generator Power Angle and Capability Curve

Further to Grainger and Stevenson (1994) examination of the generator power angle diagram re-enforces the effect inertia has on system stability. As can be seen from the power angle curve in diagram 1 there is no relationship with reactive power when considering the system stability. The system stability is directly linked to the real power of the generator. Therefore, it is reasonable to say system stability is directly related to system inertia, as inertia and power also have a direct relationship, as has already been established.

2.2.2 Inertia and Acceleration

A sudden drop in load would see the electrical power P_e reduce with the mechanical power P_m remaining constant. Even though the P_m is constant the rotor would begin to accelerate, with the mechanical inertia being the only opposition to the acceleration. An acceleration of the rotor advances the rotor angle and increases the power system frequency.

2.2.3 Inertia and Deceleration

When a load is abruptly connected the electrical power P_e exceeds the mechanical power P_m input and the accelerating power goes negative, attempting to slow the rotor. In this case, the mechanical inertia opposes the decelerating power. By opposing the change or, deceleration, the inertia minimises the frequency change of the generator.

2.2.4 Low System Inertia

As an example, if a sudden large load connects to the power system causing a disturbance where the electrical power P_e reduces suddenly, the power balance between generation and load power, the stable operation point in Figure 2.2, would be displaced. When this occurs the generator rotor will tend to accelerate as the input power from the prime mover P_m has not changed. The only dampening that counters this tendency is the mechanical inertia of the generator. A system with low inertia in this scenario would suffer power swings as the two powers P_e and P_m oscillated with no dampening.

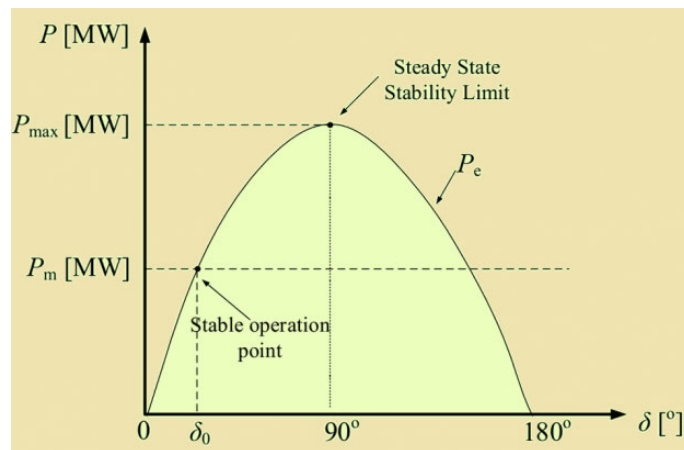


Figure 2.2. Generator power angle, (Babu, .2022)



2.3 DISTURBANCES

Grainger & Stevenson (1994) describe a disturbance as when a system is operating in a steady state condition if a sudden change or sequence of changes occurs in one or more parameters of the system, or in one or more of its operating quantities, the system has undergone a disturbance from that steady state.

Transmission faults, sudden load connection or disconnection, and the sudden loss of large generation are all considered large disturbances. Small disturbances can include altering the excitation of a generator or a tap change on power transformer. After a small disturbance occurs the system returns to the same steady state condition. If a large disturbance occurs the system will end a significantly different steady state which may be undesirable.

2.4 OPERATING STANDARDS

The following discussion on system operating standards uses the Australian energy market as an example.

The Australian Energy Market Commission (AEMC) sets system response standards in their frequency operating standard for system response requirements to large disturbances which they class as creditable and non-credible contingency events. The definitions of these events are found in the National Electricity Rules (Australia) and are summarised in the table from the AEMC Frequency operating standard (Table 2). These definitions align with the disturbance definitions found in Grainger & Stevenson (1994).

**Table 2 AEMC Frequency operating standard definition of credible and non-credible**

	REQUIREMENT	MAINLAND	TASMANIA
6	Following a <i>protected event</i> , system frequency must be maintained within the applicable extreme frequency excursion tolerance limit, and must not be outside of the applicable generation and load change band for more than 2 minutes while there is no <i>contingency event</i> , or be outside of the applicable <i>normal operating frequency band</i> for more than 10 minutes while there is no <i>contingency event</i> .		
7	Following a non-credible contingency event or multiple contingency event that is not a protected event, AEMO should use reasonable endeavours to: (a) maintain system frequency within the applicable <i>extreme frequency excursion tolerance limits</i> ; and (b) avoid system frequency being outside of the applicable generation and load change band for more than 2 minutes while there is no <i>contingency event</i> , or being outside of the applicable <i>normal operating frequency band</i> for more than 10 minutes while there is no <i>contingency event</i> .		
8	Following a <i>credible contingency event</i> (which may be a generation event , a load event or a network event), the rate of change of frequency must not be greater than...	... $\pm 1\text{Hz/s}$ (measured over any 500ms period)	... $\pm 3\text{Hz/s}$ (measured over any 250ms period).
9	Following a <i>non-credible contingency event</i> or multiple contingency events that is not a <i>protected event</i> , AEMO should use reasonable endeavours to maintain the rate of change of frequency within...	... $\pm 3\text{Hz/s}$ (measured over any 300ms period)	... $\pm 3\text{Hz/s}$ (measured over any 300ms period).
10	The size of the largest single generation event , load event or network event is limited to...	N/A	...144 MW. This limit can be implemented for an event greater than 144MW by automatic <i>load shedding</i> or any other arrangements approved by AEMO that would effectively reduce the impact of the event to 144MW or below. ¹

2.5 FREQUENCY

Power system frequency is a measurement of cycles per second with the unit being Hertz (Hz). One cycle is equivalent to one revolution of a generator rotor. This demonstrates that any disturbance to the mechanical rotation of the generator will impact the power system frequency.

According to Hou et al. (2019) frequency is one of the most important characteristics of a power system. They stress its calculation, analysis and safety and stability evaluation are of great significance to the operation of a power system. Power system frequency can be considered a real time indication of the balance between supply and demand. When the

system is balanced the frequency will be constant and remaining stable at its nominal value.

Stable frequency is essential for maintaining a stable system.

Hou et al. (2019) site the IEEE/CIGRE working group determination that frequency stability is the ability of the system to maintain or restore the frequency to the allowable range without collapse when the power system suffers serious disturbances. They further indicate that frequency collapse often cascades to large scale power transfer which could overload or fault non-fault lines, create protection mal operation resulting in system failure.

Power system frequency is constrained between tight limits. Network operators worldwide set strict limits on frequency performance. As an example, the AEMC standards (Table 3) limits specify the normal operating bands for the system frequency. The frequency must be allowed to vary slightly as system loading is never constant, with even a small load change causing a disturbance that will impact the frequency.

Table 3 AEMC Frequency operating bands

COLUMN 1	COLUMN 2		COLUMN 3		COLUMN 4
	NORMAL (HZ)		ISLAND (HZ)		SYSTEM RESTORATION (HZ)
	MAINLAND	TASMANIA	MAINLAND	TASMANIA	MAINLAND
<i>primary frequency control band</i>	49.985 – 50.015				
<i>normal operating frequency band</i>	49.85 – 50.15		49.5 – 50.5	49.0 – 51.0	49.5 – 50.5
<i>normal operating frequency excursion band</i>	49.75 – 50.25		49.5 – 50.5	49.0 – 51.0	49.5 – 50.5
<i>operating frequency tolerance band</i>	49.0 – 51.0	48.0 – 52.0	49.0 – 51.0	48.0 – 52.0	49.0 – 51.0
<i>extreme frequency excursion tolerance limit</i>	47.0 – 52.0	47.0 – 55.0	47.0 – 52.0	47.0 – 55.0	47.0 – 52.0

Note: 1. The Reliability Panel has not determined separate frequency bands for periods of **system restoration** in Tasmania.



2.6 NEW GENERATION

2.6.1 Renewable Energy Sources

As the world moves towards more sustainable sources of energy the development of Renewable Energy Sources (RES) has accelerated exponentially. RES are defined as sources that can replenish their source naturally over a period of time, some examples of RES include:

- Solar/ photovoltaic
- Wind
- Biomass
- Geothermal

These technologies use a naturally occurring resource and convert the energy they create into electrical energy to connect to the power system.

2.6.2 Battery Energy Storage Systems

Another form of technology developed to meet sustainable criteria is the Battery Energy Storage Systems (BESS), this differs from RES as it contains banks of rechargeable batteries as its source.



2.7 INVERTER BASED RESOURCES

For this project discussion involving RES or BESS will consider them to be large scale direct grid connected units, this does not include domestic scale systems.

Both BESS and RES use a power electronic stage to convert their source of energy to a grid compatible AC source e.g., a BESS is a DC source. Using an inverter or power electronic interface for connection is commonly referred to as Inverter Based Resource (IBR). Large scale IBR that connects to a power system can be broken into two groups, firstly Grid Following Inverters and the other Grid Forming Inverters.

2.7.1 Grid Following Inverters

Grid following inverters (GFL) use a control system that measures and synchronises to the power grid voltage waveform which then adjusts the inverter power output to follow the network voltage (AEMO,2023). GFL require a reference voltage signal from other generators to operate successfully. If the reference voltage is lost the GFL will shut down. GFL inverters can provide some network support autonomously by adjusting their output voltage and frequency however, during a disturbance their response is controlled and dependant on provider settings. The speed of the response can be limited and there are further concerns with stability where a high penetration of inverters is connected to the network.



2.7.2 Grid Forming Inverters

Grid Forming Inverters (GFM) use a control system that can set internal voltage waveforms and adjust their own power output independent of network connection. GFM have no reliance on external grid voltage to maintain operation, so they can operate independently with or without other generators on the network. GFN inverters can inherently help stabilise network fluctuations by very rapidly adjusting their power output and can self-maintain their frequency. There is a considerable amount of effort and research going into GFM control systems at present with a vast number of trials underway internationally and here in Australia. (AEMO, 2021)

2.7.3 IBR and Inertia

Unlike the electromechanical coupling found between the mechanical power and the electrical power of a synchronous generator, IBR has no direct coupling between the source and the electrical power exported to the network. This is due to the power electronic interface that is inherent in all IBR. As there is no electromechanical link between the source and the power exported from IBR it means that it is not capable of providing the same inertial response as that of a synchronous generator.

Research has shown that grid forming inverters can provide a form of inertia as long as they are connected via an energy storage device such as batteries (BESS). This type of inertia is referred to as synthetic inertia which, is the operation and coordination of the power electronic interface to mimic the output characteristic of a synchronous generator during a disturbance.

(AEMO) indicate that a synthetic inertia response, to be successful, must be inherently operated or initiated and be sufficiently fast enough and large enough to help manage Rate of Change of Frequency (RoCoF). For synthetic inertia to successfully operate, the initial response requires an energy buffer with adequate headroom and footroom to facilitate a fast exchange of energy with the grid following a disturbance.

A limiting factor of synthetic inertia can be the overcurrent settings of the inverter which can be considerably lower than the over current setting found in a synchronous machine (AEMO). This limiting factor can inhibit the inverter's response if that inverter is operating near its rated capacity already. This results in differing levels of contribution from the IBR during a disturbance.

The inertial response from IBR using synthetic inertia is sensitive to the control system design. The inertial control parameters for synthetic inertial response may be set differently by various manufacturers or service providers and maybe implemented differently in the design.

As an example, Tielens discusses how wind turbines may very well have an amount of kinetic energy available stored in the blades, gearbox, and generator. The inertia constant of the wind turbine depends on its type, size and whether it has a gearbox installed or not. In general, a wind turbine does have mechanical inertia or kinetic energy stored via its blades and its generator. This could be somewhere in the order of three to six seconds which is comparable with conventional synchronous generation plants. However, it is important to note that the inertia constant for a wind turbine is defined at its nominal speed so with varying speed due to different wind conditions this inertia constant will change. Tielens goes



further and observes that even how the wind turbine is operated will change this value. To maximise the power output of the wind turbine at low speeds the rotor speed is decreased which will have the consequence of producing less kinetic energy or inertia. (Tielens and Van Hertem, 2015)

2.7.4 Location Concerns

Xu et al(2018) highlights that power system inertia can be limited by locational factors with a particular focus on constraints in Power transfer due to line capacity. When lines have limited capacity, they can restrict the amount of power that can be transferred between different parts of a network. This limitation can reduce the overall inertia available in that system as the power balance cannot be restored due to that constraint. Through modelling Xu et al.(2018) Demonstrated that the impacts of inertia on system oscillation behaviour vary by the inertia's location.

2.8 RATE OF CHANGE OF FREQUENCY (ROCOF)

A substantial amount of literature was reviewed for this project, the majority of which states the accepted method of analysing the performance of system frequency is via the application of the Rate of Change of Frequency (RoCoF) calculation.

ENTSO-E (2020) State the most important indicator of the health state of the power system inertia is by examining the frequency stability using RoCoF. Further, it stresses that fixing maximum RoCoF limits for electrical power systems means determining the maximum stress that it can sustain and survive; this implies that under these conditions all control



loops, active power control, and protection systems including defence systems are able to trigger and react in accordance with their system governance settings. ENTSO-E,(2020). Tielens and Hertem (2015) highlight that in literature, even though different methods are used to study system inertia or estimate system inertia, in principle they all lead back to using RoCoF.

RoCof is the time derivative ($\Delta f/\Delta t$) of the power system frequency and is an important quantity that qualifies as the robustness of an electrical grid. The initial value of the derivative is the instantaneous RoCof just after an imbalance of power in the electrical power system before the action of any control ENTSO-E.(2020). RoCof calculations can either focus directly on the frequency deviations or include consideration of how the changes in the power system also impact the system frequency. For a real-time determination of RoCof it is possible to use two different approaches however, one is more difficult due to the data required.

The formula for RoCoF that focuses on free frequency deviations directly:

$$\mathbf{RoCoF} = \frac{\Delta f}{\Delta t} \quad (2.12)$$



The equation that considers changes in the power in the system

$$RoCoF = \frac{(\Delta P) \times f}{2 \times S_n \times H} \quad (2.13)$$

Where,

ΔP – change in power (MW)

S_n – Rated apparent power of the system (MVA)

As can be seen, using (2.13) would require knowledge of the instantaneous power at that point in time and the inertia constant of the entire system, making it impractical for a real time calculation as loads on the network change frequently and indiscriminately. However, this equation is useful for post-event analysis when the data can be recovered from event captures.

The initial $\Delta f/\Delta t$ is the instantaneous RoCoF just after the disconnection of either a generator or load from a power system. This is theoretically the highest system RoCoF. ENTSO-E., (2017).

2.8.1 RoCoF Performance

Transmission operators establish performance standards for RoCoF in transmission networks. As an example, in the AEMC standard, there are performance requirements for the frequency during large or small disturbances or credible or non-credible events. Of main interest is the RoCoF performance requirement, see Table 4.

**Table 4 AEMC Frequency operating standard for RoCoF**

	REQUIREMENT	MAINLAND	TASMANIA
6	Following a <i>protected event</i> , system frequency must be maintained within the applicable extreme frequency excursion tolerance limit, and must not be outside of the applicable generation and load change band for more than 2 minutes while there is no <i>contingency event</i> , or be outside of the applicable <i>normal operating frequency band</i> for more than 10 minutes while there is no <i>contingency event</i> .		
7	Following a non-credible contingency event or multiple contingency event that is not a protected event, AEMO should use reasonable endeavours to: (a) maintain system frequency within the applicable <i>extreme frequency excursion tolerance limits</i> ; and (b) avoid system frequency being outside of the applicable generation and load change band for more than 2 minutes while there is no <i>contingency event</i> , or being outside of the applicable <i>normal operating frequency band</i> for more than 10 minutes while there is no <i>contingency event</i> .		
8	Following a <i>credible contingency event</i> (which may be a generation event , a load event or a network event), the rate of change of frequency must not be greater than...	... $\pm 1\text{Hz/s}$ (measured over any 500ms period)	... $\pm 3\text{Hz/s}$ (measured over any 250ms period).
9	Following a <i>non-credible contingency event</i> or multiple contingency events that is not a <i>protected event</i> , AEMO should use reasonable endeavours to maintain the rate of change of frequency within...	... $\pm 3\text{Hz/s}$ (measured over any 300ms period)	... $\pm 3\text{Hz/s}$ (measured over any 300ms period).
10	The size of the largest single generation event , load event or network event is limited to...	N/A	...144 MW. This limit can be implemented for an event greater than 144MW by automatic <i>load shedding</i> or any other arrangements approved by AEMO that would effectively reduce the impact of the event to 144MW or below. ¹

The assessment time differs depending on the contingency. The shorter measurement times e.g., 500ms, provide a more sensitive detection of rapid changes in the frequency and detection of disturbances. The result of the shorter measurement period can be prone to fluctuations that aren't associated with a disturbance and possibly could be attributed to a load change etc. To filter out unnecessary noise the measurement is assessed over a one second period. Figure 2.3 (Chown Et al.,2017) displays how an overly sensitive measurement period will yield a result that would not meet the standard. In this figure, a measurement taken over a 100ms window would erroneously indicate a RoCoF value of 3 Hz/ s. This assumes that this would be a credible contingency event, hence the 500ms assessment.

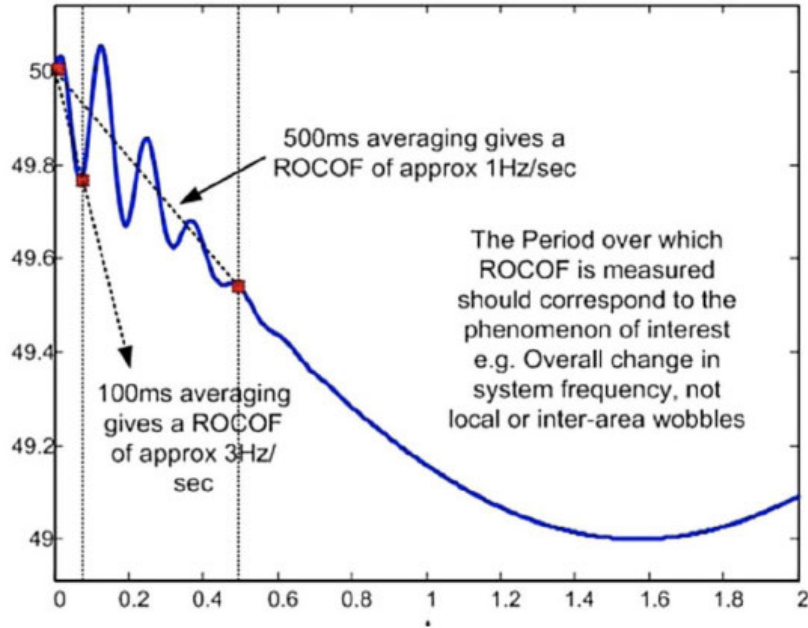


Figure 2.3. Example of RoCoF measurement and assessment
(Chown Et Al., 2017)

2.9 SCADA

Literature reveals ongoing research into the use of Scada for the determination of inertia over a period. The result of this type of analysis would be suited to trending the variation in inertia with respect to the change in load and generation conditions and could be used to assist in identifying potential areas of shortfall in inertia. Being a trending tool it would not necessarily be suitable for real time measurement. The system is reliant on knowing the inertial constant of each generator and the state of service of that generator on the system knowing these two values it allows the determination of what synchronous generators are in service at what time and what the load is at those times i.e., equation (2.13).

The result of this calculation using a SCADA method can be seen in figure 5 (ENTSO-E. 2020). This is an example from an Italian system, over a typical three-day period, of the trend of inertia versus the total demand and the RES versus total demand for the same period.

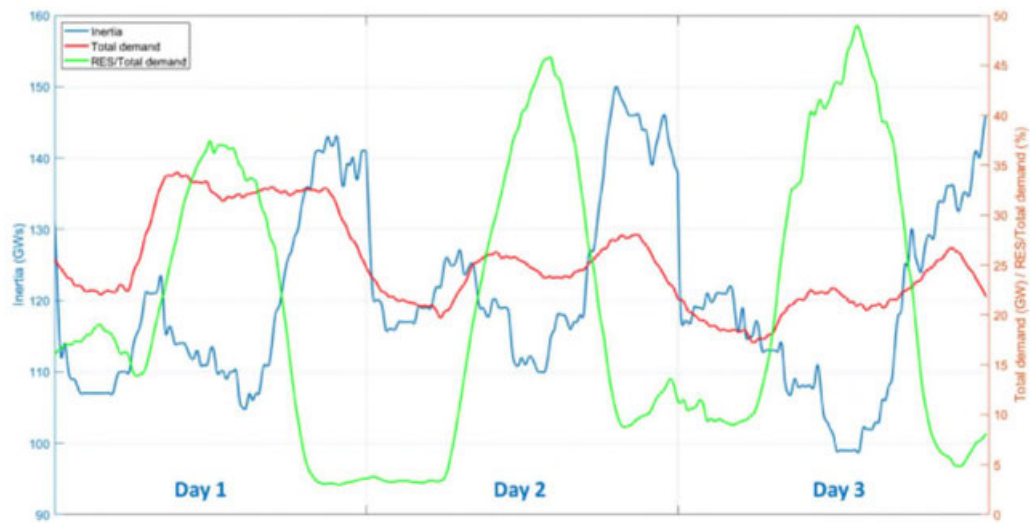


Figure 2.4. Example of an Italian system during a three-day period (ENTSOE-E. 2020) Inertia and Rate of Change of Frequency (RoCoF)

The result in figure 2.4 clearly demonstrates an inertia shortfall when there is a high penetration of RES/ IBR in the system.



2.10 CHAPTER SUMMARY

In respect to objective 1.4.1 it has been established that the displacement of synchronous generation by RES will impact the historical levels of inertia in the power system. The research has revealed this is a concerning and emerging problem worldwide with ongoing research continuing. There is some promising technology being developed with the capability of injecting synthetic inertia however, this is still in the development and testing stages.

It has been established that examination of system frequency, using RoCoF criteria, is an excellent method of determining the system inertia in real-time due to its direct relationship with the mechanical inertia of the generator.



CHAPTER 3 METHODOLOGY

The following will detail the methodology used to simulate a real time analysis of power system inertia in a power network. The network model and the associated code will be outlined in this chapter. The reasoning and selection and modification of various parts of the model and the code will also be discussed.

3.1 SIMULINK MODEL

The model used in Simulink was developed over several iterations. Initial design considerations included modelling a grid following Bess in parallel with several synchronous generators. Considering the purpose of the project was examining the system inertia and that GFL BESS is not capable of providing the inertial response, it was decided to remove the extra complexity of this design. Instead, the focus was on accurately modelling what can provide inertia and assessing it.

The Simulink model can be found in figure 3.1. This model was reconstructed based on the example in the MathWorks training module and consists of two synchronous generators in parallel connected via circuit breakers so they could be switched out to simulate various conditions on the network. The generators supply a fixed active load, a fixed reactive load, and a variable load. The variable load will have staged controls so active loads could be added or subtracted from the system again to mimic system conditions.

This model will be a reasonable estimation of a worst-case scenario with the introduction of IBR as it will model when the renewable resource is unavailable, due to either being

exhausted or weather impacted, and the system is being supported by synchronous generation only.

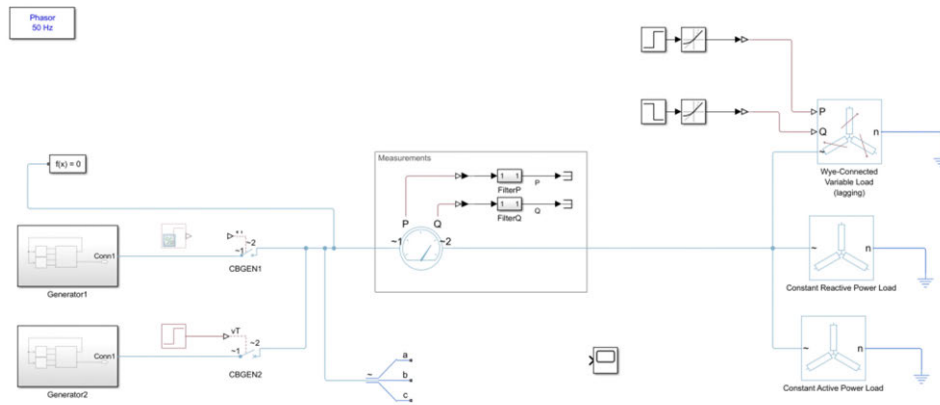


Figure 3.1 Simulink model (based on Mathworks Model)

3.1.1 MODEL COMPONENTS

3.1.1.2 Generators

The generators consist of three main components firstly there's the generator itself which is shown as a synchronous generator. Both round rotor and salient pole generators are examined in the modelling. Both are reasonably common in generation with round rotors used in more robust, higher speed operation e.g., steam turbines, and Salient pole generators used in lower speed operation, typically hydropower applications.

The generator model includes a per-unit connection which uses a reference from the voltage of power output for feedback to the generator control. It contains f_d positive and f_d negative connections for field terminals that connect to the exciter, and it has R and C inputs which

relate to the governor and control signals for regulating the generator's speed and power output, see figure 3.2.

3.1.1.3 Automatic Voltage Regulator

The automatic voltage regulator (AVR) automatically adjusts the voltage output of the generator by controlling the exciter which ensures the generator maintains a constant voltage as load changes. It has an input directly connected to the output voltage of the generator and adjusts the excitation by the fd positive and fd negative terminals (figure 3.2).

3.1.1.4 Prime Mover and Governor

The prime mover represents the mechanical input, traditionally a steam turbine or diesel generator, that drives the shaft of the generator. The governor controls the speed of the prime mover to maintain the frequency to a set limit. There are two reference signals for the governor, R and C and a reference from the voltage output in per unit these are used as controlled loops to regulate speed and power, (Figure 3.2).

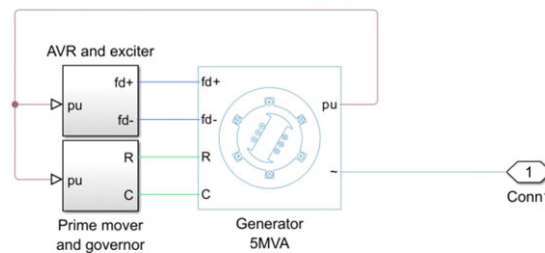


Figure 3.2. Generator block



3.1.1.5 AVR and Exciter Block

Examining the AVR and Exciter block reveals the controls for the reactive power regulation and voltage control of the synchronous machines field circuit.

The system has a voltage feedback loop which measures the input voltage in per unit from the generator $v_{gen\ 1}$ and compares this to a voltage reference V_{ref} by a comparator. The value of V_{Ref} is the desired output voltage for the system, in this case 1 pu (see figure 3.3).

The system also has a feedback loop for the reactive droop control $Q1$. A signal representing power output $Q_{Gen\ one}$ is fed into a droop control mechanism $droop\ Q1$. Droop control is used to adjust the generator's output in response to changes in load and helps balance reactive power while ensuring voltage stability. The droop control introduces a proportional relationship between the reactive power output and the voltage deviation. This control was not adjusted during the simulation as it has no real impact on the system inertia.

The next main stage of the system is the voltage control block. This block processes the output of the comparison between V_{ref} and V_{Gen} and accounts for any group setting. The output of the voltage control block generates an excitation voltage signal (E_{fd}) which regulates the field current of the synchronous machine, this adjusts and controls the generator's output voltage, by adjusting the machine's rotor magnetic field strength.

The synchronous machine field circuit generates the field current required for the machine based on the field excitation value E_{fd} . The I_{fd} per unit is not utilised in this system so it is terminated.

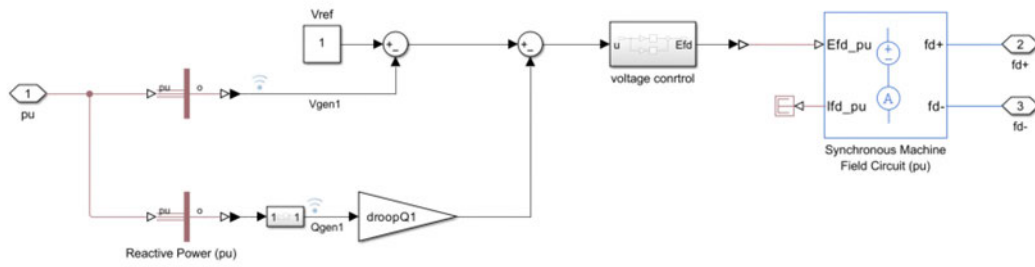


Figure 3.3 Voltage control block

3.1.1.6 Prime Mover and Governor Block

The prime mover and governor block is like the AVR exciter block in that it contains two comparators on the system feedback (Figure 3.4).

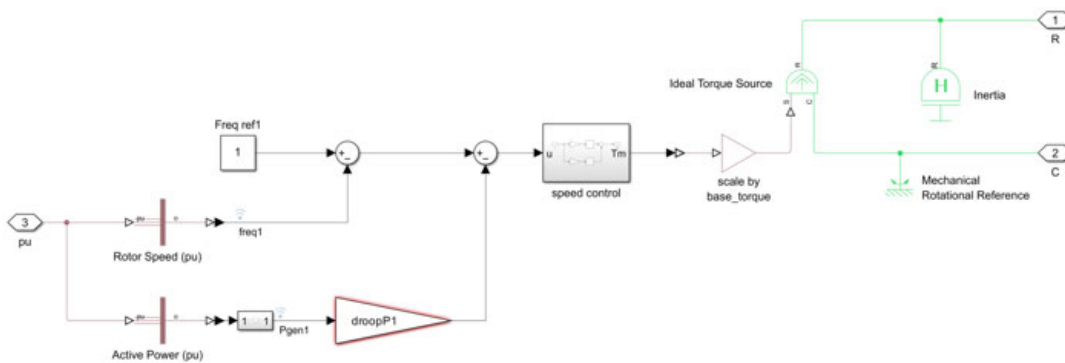


Figure 3.4 Examination of governor control block

The speed of the rotor is measured in per unit (freq1) and is an important variable as this directly represents the frequency of the generator. This variable is then compared with the frequency reference frequency reference one which is the nominal frequency desired. The comparator establishes the error between these two values, and this is fed then into the speed control system.



The next control is the active power control loop, the active power represents the portion of power that performs useful work, and this is directly related the torque and speed of the generator. The active power feedback is connected to the group control setting droopP1. The droop control helps to regulate the generator's active power by managing the speed set point. The set point is adjusted in line with the network settings to enable a predetermined value of power to be input into the system by the generator. Like the frequency comparator, the droop comparator adjusts for the error between the actual power and the desired power and sends this to the speed controller.

After receiving the error between the reference frequency and the actual rotor frequency or speed, the speed control adjusts the mechanical torque applied to the generated rotor to minimise the error. The mechanical torque output from the speed controller is effectively the torque that is applied by the prime mover to the rotor of the generator. There was a direct relationship between this torque and the active power generated by the machine. The speed control block controls the prime mover such that the correct torque is applied to maintain a constant speed and hence constant frequency.

The torque scaling block adjusts the mechanical torque to the base torque of the system. The ideal torque source is a block that represents an ideal torque. It generates torque at its terminals proportional to the input physical signal. The source block is ideal in the sense that it is assumed to be powerful enough to maintain specified torque regardless of the angular velocity at the source terminals (MATLAB block Parameter). The H block or inertia represents the inertia of the rotating mass of the generator, this block includes the inertia coefficient representing how much kinetic energy is stored in the rotor.

The mechanical rotational reference establishes the desired rotational speed of the generator rotor. This is set in revolutions per minute or in per unit value, effectively this is the target for the prime mover to control the rotational speed of the generator. The two outputs labelled R and C are connections which perform the resistance and dampening of the machine and will affect the generator's response to the change in speed.

Both the AVR and exciter Block and the Prime Mover and Governor Block contain a PI control block. Where the input signal is passed to both a proportional path and an integral path. This path applies a gain and passes this directly to the summation block where the integral path multiplies the input by the same gain and passes it through a discrete integrator to accumulate the input signal over time. Both these outputs are summed together to create an output which adjusts the mechanical torque in the generator (figure 3.5). The above description applies to both generators in this system.

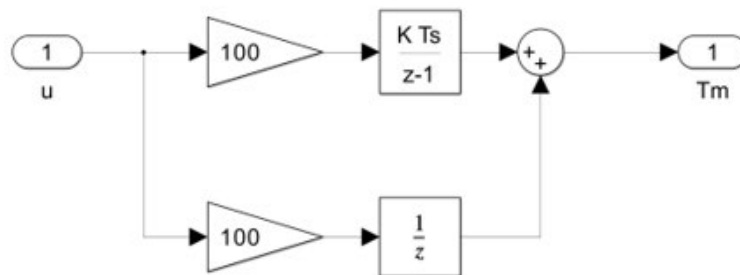


Figure 3.5 PI control used in AVR and governor blocks

3.1.1.7 Network Components

Each generator is connected via a circuit breaker to the network however, to avoid a total loss of supply, only one of the circuit breakers will operate during the simulation, being CBgen2. The circuit breaker switching is controlled via a timed step input.

The measurement block extracts the active and reactive power from the system and outputs these values for data analysis. These signals are connected through a discrete integral block to filter out any high frequency or noise from the system and just pass the steady state component only of each of the signals to the data handler.

The load connected to the network consists of a fixed active load, a fixed reactive load, and a variable load. The variable load has inputs for the active and reactive load it controls. The load can either be added or removed from the system with this load block. These inputs are activated by two-step controls that run through individual rate limiters. The rate limiters are there to provide some ramping to the step control. This is designed to mimic a load change on the network. The step change for the load coming on occurs at a pre-determined time after the initiation of the simulation. The settings for the various components can be found in the appendices.

3.2 MEASUREMENT OF ROCOF

3.2.1 Zero Crossing

A simple method that establishes the system frequency is to take time difference measurements between known equidistant points in a waveform. The most logical and



attainable point is the zero crossings of the time axis of a voltage waveform. For accurate and reliable frequency measurement more than two points or zero crossings should be measured. For one full cycle, there are three zero crossings, so the method involves a sliding window measuring every half cycle i.e. two points. Changes in frequency would result in a change in the measured time of each half cycle. The result would then be assessed with any deviation being further analysed against the RoCoF standards. The issue with a simple zero crossing measurement is that noise or high harmonic content can interfere with the voltage waveform as, if the noise is severe enough it can provide erroneous zero crossings, distorting the measurement window. (Serov et al, 2021.). Serov et al. examined several techniques for removing the noise from the frequency and gaining a clear zero crossing measurement including piecewise linear approximation, least squares technique and input filtration.

3.2.1.1 Piecewise

Piecewise linear approximation applies an approximation of the frequency near its zero crossing to reduce the methodical error component. It is a method of improving the measurement resilience against unwanted noise. It uses first-order polynomials to create a linear approximation at zero crossing points. Essentially this method determines the zero crossing just before and just after the zero crossing and joins them with a straight line. This provides the zero-crossing point (figure 3.6).

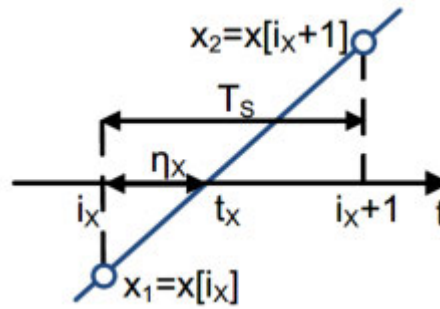


Figure 3.6 Piecewise linear approximation of the zero-point crossing (Serov et al. 2021)

3.2.1.2 Least Squares

The least squares technique determines the coefficients of the polynomial. This minimises the impact of any noise in the frequency and finds the best fit based on multiple samples around the zero-crossing point. This method is computationally heavy.

3.2.1.3 Input Filtration

Serov suggests this method applies a low pass filter to remove unwanted noise from the frequency. Ideally if successful this method would remove all frequencies and unwanted spectral noise from the fundamental component.

3.2.2 Discrete Fourier Transform

From 3.2.1.3 Serov et al. suggests using a Discrete Fourier Transform (DFT) to filter the noise form from the waveform and return the component values. This method translates time domain voltage waveform into the frequency domain by a fast Fourier transform analysis (FFT). This can determine the frequency using the well-known Fourier analysis technique. This method makes it possible to determine the frequency using only a section of the waveform. (Chown et al.,2023)

The discrete Fourier transform technique was chosen for this project. The concept is that if the DFT could successfully break down a waveform with a significant harmonic effect and identify all the frequencies involved, a filter could be applied with a relatively tight constraint around 50 Hertz which could isolate the fundamental frequency from the noise.

3.2.3 FFT

The FFT is an equivalent representation of the voltage waveform in the frequency domain rather than the time domain and breaks the signal down into its discrete frequencies (Seeber & Ulrici. 2016). The DFT, uses a FFT, is a transform that decomposes the voltage waveform into two sinusoids:

- Cosine waves - these represent the real part of the transform
- Sine waves - these represent the imaginary part of the transform

These two sinusoids are orthogonal to each other which enables the transform (DFT) to isolate component frequencies. The DFT projects the voltage waveform onto a set of basis functions, sine and cosine waves of different frequencies that can be expressed as complex exponentials each of which represents a specific frequency (equation 3.1). The voltage waveform is broken down into contributions of each of these basis functions. Because the basis functions are orthogonal, it enables the DFT to clearly distinguish the contribution of each frequency to the overall waveform, with no overlap between differing frequencies.

$$e^{j\omega t} = \cos(\omega t) + j\sin(\omega t) \quad (3.1)$$

Where,

e Euler's number

j Imaginary unit

ω Angular frequency

t time

$\cos(\omega t)$ Real part of the complex exponential function

$j\sin(\omega t)$ Imaginary part of the complex function

Figure 3.7 displays a geometric representation of the orthogonal decomposition of a frequency (Seeber & Ulrici. 2016).

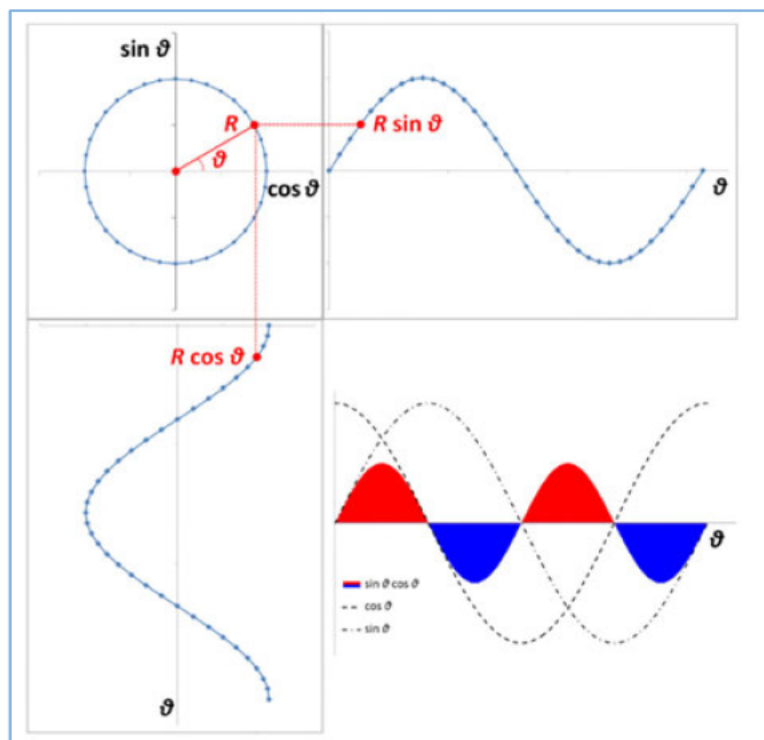


**Figure 3.4 Orthogonal decomposition of a waveform
(Seeber & Ulrici. 2016).**



The DFT returns two results for each frequency present, one a positive frequency and the other a negative frequency which, is a mirror of the positive frequency. These results indicate the component frequency and its amplitude. The amplitude of both positive and negative values is half of the actual amplitude of the analysed frequency. For analysis, the negative frequency can be ignored, and the amplitude of the positive frequency just doubled. However, any reconstruction of frequencies from a DFT must use both positive and negative results. The analysis completed uses the positive component by adjusting the range of the result. These values are then doubled, excluding the first result, the DC component and the last result, The Nyquist value.

The resulting frequencies are then filtered to between a desired range, isolating the fundamental frequency; in the case of a nominal 50 Hz frequency network, the range may be set to between the frequency operating standard values of the network operator e.g. 49 - 51 Hz. MATLAB will be used to apply a DFT to the frequency as the FFT function is in-built.

3.2.4 Three Level DFT

A method to improve the accuracy was suggested by Nam et al. (2015), that of applying a three level DFT. As the name implies three stages of DFT are applied to the original waveform which the paper indicates produces a more accurate and stable frequency estimation compared with a single-level DFT as it can help avoid spectral leakage, where the resultant frequencies from the transform creep into adjacent frequency bins.



Being a multistage process there is an additional two-cycle delay due to the extra computations, although the authors are confident that it will still be quick enough to be used for rapid response applications. Time permitting this method will be modelled for comparison to the single DFT technique modelled.

3.2.5 Sliding DFT

Numerous research pieces indicate a DFT is susceptible to the influence of input noise. The research suggests techniques for further refinement of the DFT to improve the accuracy of the result. Serov et al. (2021) suggests using a sliding DFT as an input bandpass filter. This suppresses noise and non-fundamental spectral components with the sliding DFT applied over half-cycle periods i.e., one every 10ms for a 50 Hz waveform, or overlapping windows. The technique continuously renews the transform with updated spectral information as new data points are measured. Like the DFT discussed earlier this method filters out high-frequency components and non-fundamental harmonics. This means the sliding transform is useful for a dynamic measurement of the frequency, as it is not restricted to a discrete period.

3.3 ROCOF

From the result of the sliding DFT the resultant fundamental frequency will be analysed. Any excursions outside the predefined limits as per the Frequency Operating Standard will trigger a RoCoF event. The code will execute the calculation and will return a text message in the command window stating the time and value of the RoCoF event.



3.4 NYQUIST FREQUENCY

When sampling the frequency, the sampling rate will be set well above the Nyquist frequency. This will be adjusted down once successful measurements have occurred to improve computational efficiency. (Seeber & Ulrici. 2016) state sampling at a rate much higher than the minimum value fixed by the Nyquist criterion will yield the original signal with quite good accuracy when re-constructed. Further they indicate that if the sampling rate was equivalent to the Nyquist criterion the interpolation to reconstruct the signal would be computationally heavy.

3.5 CHAPTER SUMMARY

The methodology proposed will meet objectives 2,3 and 4. Several different methods were sourced through the research. The technique selected will apply a sliding DFT to analyse a voltage waveform modelled in a simulated network. The output of the DFT will be analysed and event captures will trigger for any RoCoF events. A message will be generated that, in a real-world application, alerts a system operator to a RoCoF event.



CHAPTER 4 RESULTS AND DISCUSSIONS

As detailed in the methodology section a simulated network was developed in Simulink to investigate the system frequency response to varying conditions. Appendix B includes further discussion of individual components of the model. The intention of the modelling was to use Simulink to run a network model and have the dynamic inertia monitored in real time using MATLAB codes, found in Appendix C. This integration was not successful, so the model was broken into component parts for the research and analysis.

The first section of the results details the operation of the model and examines the result. The second main section of the results details the MATLAB codes used to generate example waveforms and frequency profiles. These are then analysed to determine the success of the methodology.

4.1 SIMULINK NETWORK MODEL

The network model overview can be found in figure 4.1. This model was used for all testing as part of this research, with the results produced using the data inspector tool. Parts of the setting data for the generators were sourced through MATLAB. This gave the ability to alter settings relatively easily for different scenarios e.g., droop control settings.

The simulations completed as part of the analysis were:

- A small disturbance with both generators in service
- The same disturbance but the droop setting adjusted on one generator
- A large disturbance with both generators in service
- A large disturbance with the addition of a generator trip
- A change in generator type

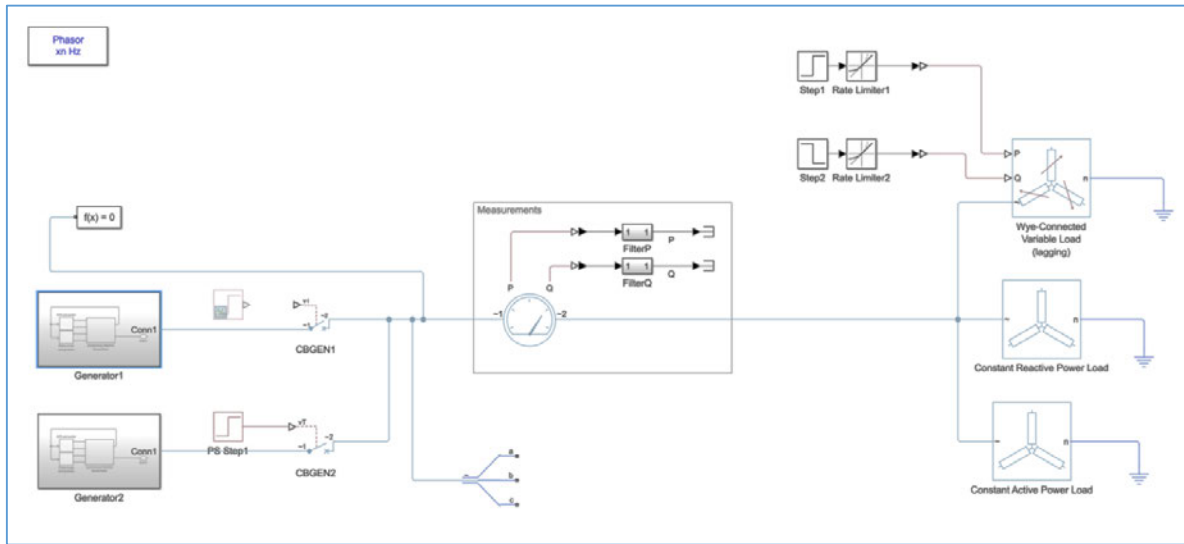


Figure 4.1. Simulink Model

Most of the testing was completed using the round rotor generator. This generator is specified as a four-pole generator running at 1500 rpm, a typical speed of a 4-pole synchronous generator. For a 50 Hz system, the calculation is equation (4.1)

$$\eta_{syn} = \frac{120 \times f}{P} = \frac{120 \times 50}{4} = 1500 \text{ RPM} \quad (4.1)$$



4.1.1 Model Tests

The following six tests were completed using the model to demonstrate the behaviour of the system frequency during different events. The system is deliberately weak for testing and analysis purposes. The tests conducted are as found in Table 5.

Table 5 Tests completed using Simulink model

Test	Generator	Load	Condition
1	1 & 2	200 kW	Load closed in at 3 sec
2	1 & 2	200 kW	Load closed in at 3 sec with generator 1 set to 1% droop
3	1 & 2	4MW	Load closed in at 3 sec
4	1 & 2	4MW	Load closed in at 1 sec & Generator 2 trips at 3 secs
5	1 & 2	4MW	Load closed in at 1 sec & Generator 2 trips at 3 secs Generators are salient pole type
6	1 & 2	4MW	Generator 2 trips at 1 sec & load closed in at 3 secs

4.1.1.1 Test 1. Small Disturbance

A small disturbance was applied, via the variable load step, closing a 200 kW resistive load after three seconds. In this scenario both generators remain in service throughout the 10-second window, both having a 3% droop setting.

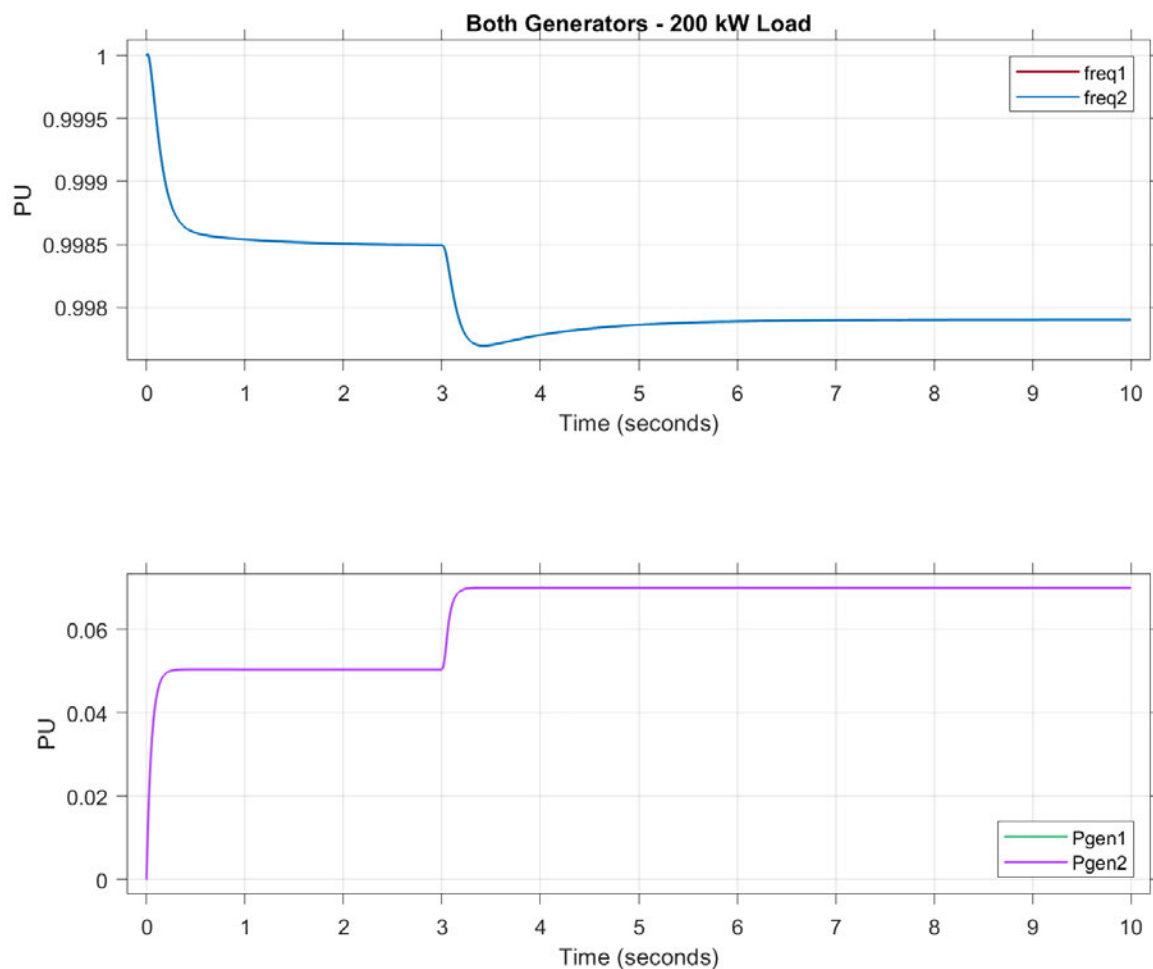


Figure 4.5. Test 1 small disturbance

The initial dip, zero seconds to approximately one-half a second, in the frequency is where the generators energise the fixed loads. As can be seen in Figure 4.2, the system can be considered to have adequate inertia to ‘ride through’ this disturbance at three seconds.

4.1.1.2 Test 2. Droop Adjustment

The same simulation was run as per test 1 however, the droop was altered on generator 1 to 1%.

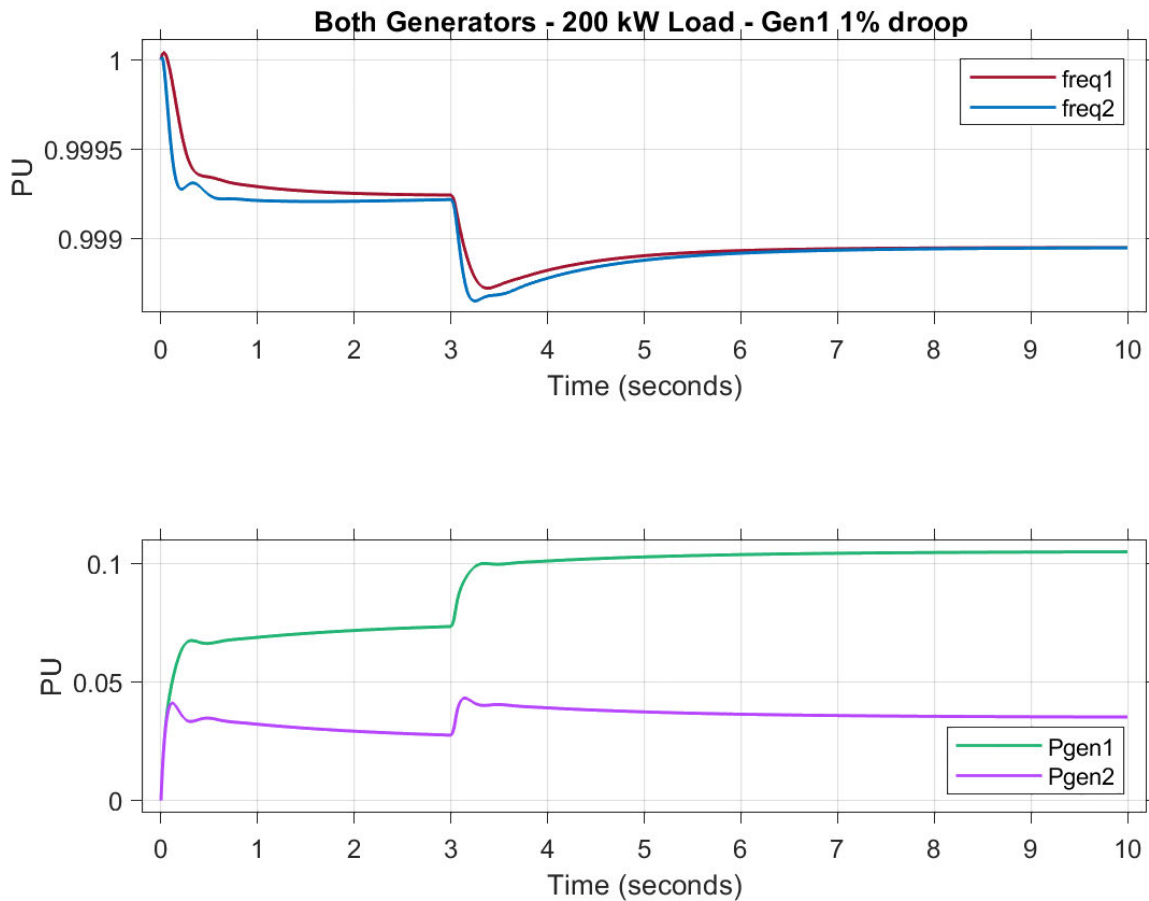


Figure 4.6. Test 2 demonstration of droop setting change

By inspection it can be seen there is a slight change in behaviour, however the inertial response remains relatively unchanged. This demonstrates there is no correlation between system inertia and droop settings.

4.1.1.3 Test 3. Large Disturbance

A large disturbance was applied, again via the variable step, closing a 4 MW load after one second. As per test one, both generators remain in service throughout the 10-second window, with a return to the 3% droop setting.

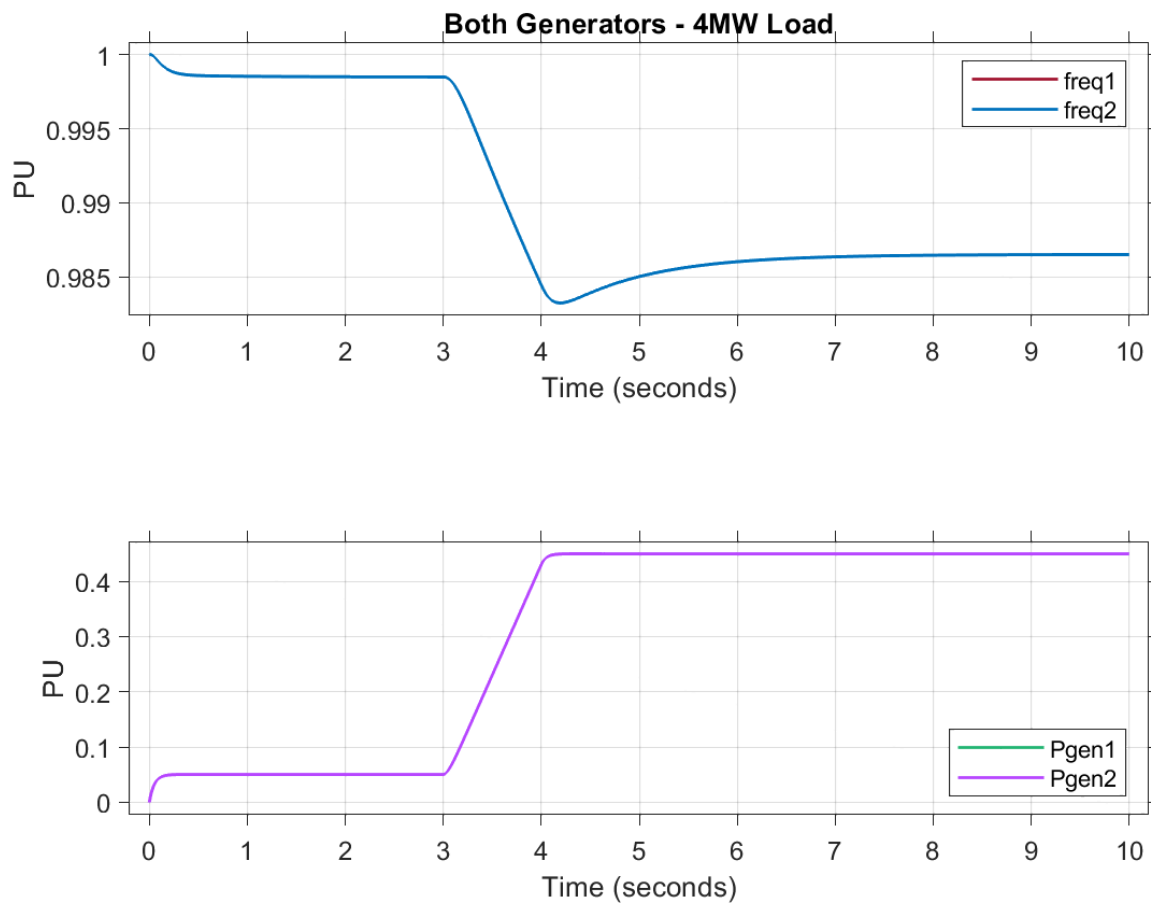


Figure 4.7. Test 3 Large disturbance test

This can be considered a best-case scenario for this load change as no further disturbances occur during the test. This test demonstrates the definition of a large disturbance as found in the frequency operating standard, being a sudden load change.

4.1.1.4 Test 4. Large Disturbance and Loss of Generator

In this test, the same 4 MW load is closed in after 1 second. In addition, generator 2 trips after 3 seconds.

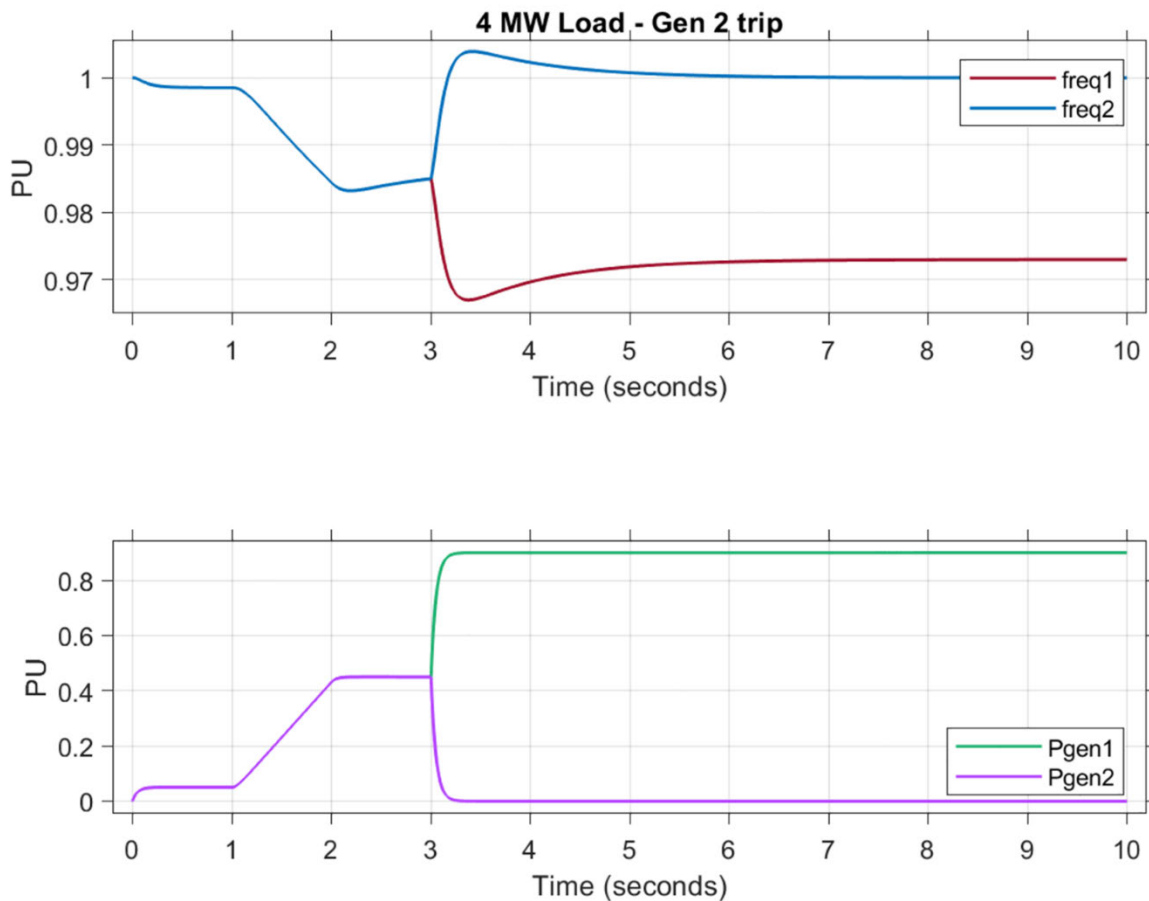


Figure 4.8. Test 4 Large disturbance and loss of generation

The associated dip in frequency for the second disturbance is severe. This simulated another definition in the frequency standard, being a loss of generation. It can also be observed that the tripped generator, generator 2, experiences an overshoot in its recovery, attributable to the sudden imbalance in prime mover power and load power balance. Generator 2 over speeds until its own control system can respond.

4.1.1.5 Test 5. Salient Pole Synchronous Generator

The generator type was changed to a salient pole type for the next demonstration. In this test, the same parameters were applied as those in test 4.

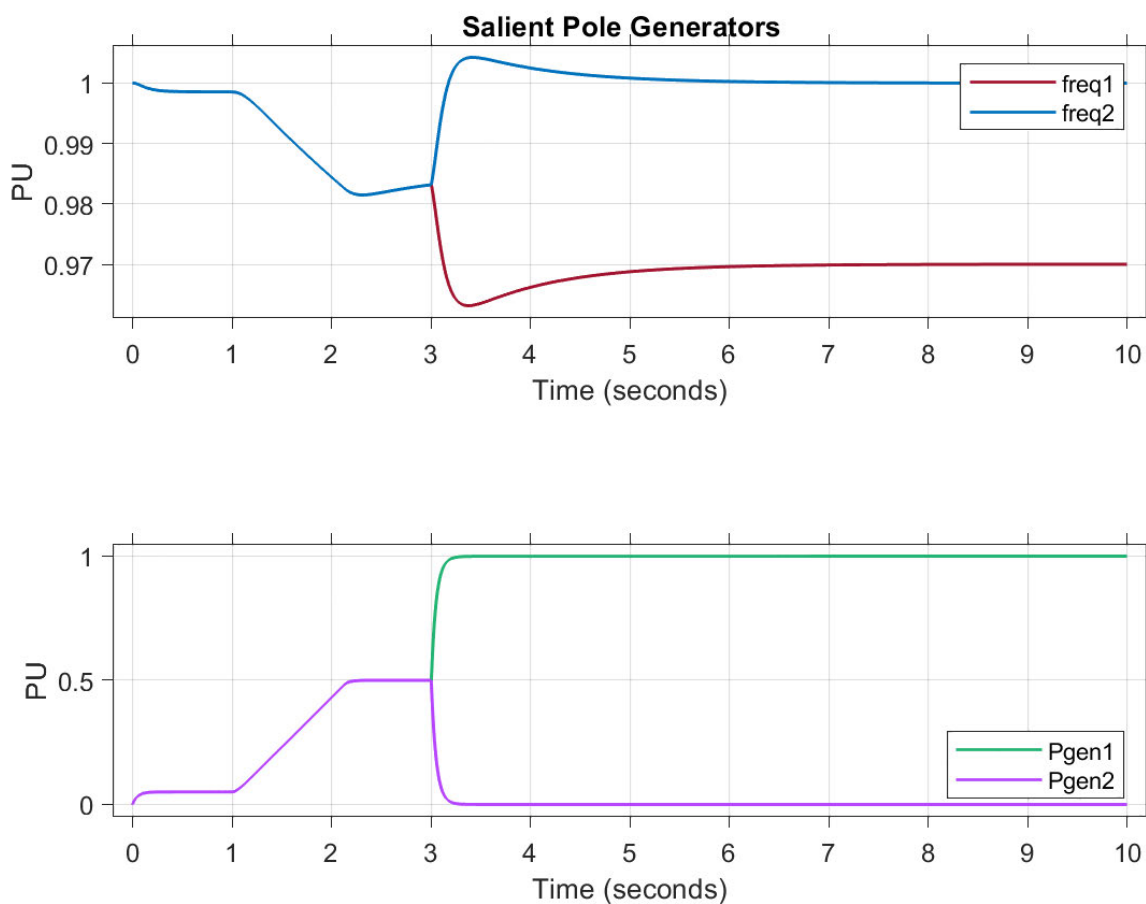


Figure 4.9 Test 5 Salient pole generators

Similar dips in the frequency are observed when using salient pole generators, with the loss of generation dip dropping further than the same for the round rotor.

4.1.1.6 Test 6. One Synchronous Generator

Loss of one generator at one second with a large disturbing load connecting at three seconds.

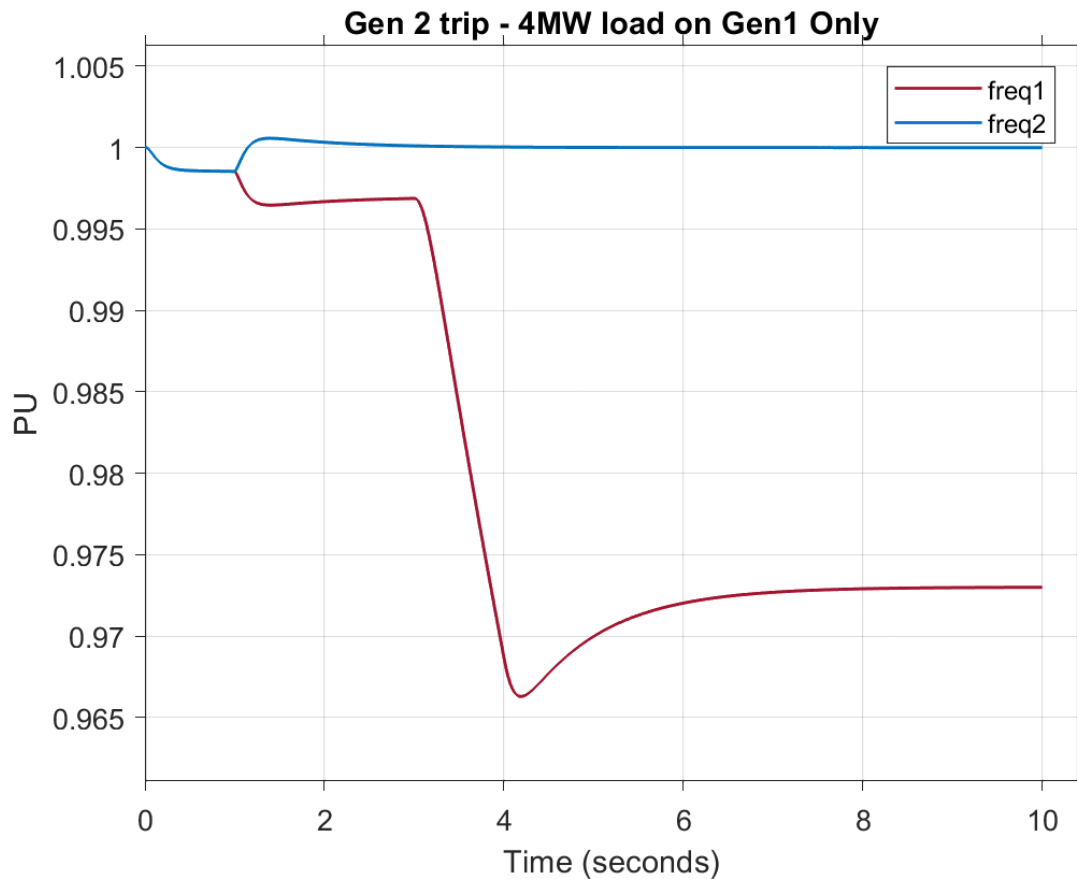


Figure 4.10 Test 6 simulation of a lack of inertia

The intention of this test is to focus on the inertial response to the load disturbance at three seconds. This simulates the scenario where there may be RES connected but does not provide system inertia as it is set as a grid following unit.

4.1.2 Summary of Simulink Results

Two tests were further examined with data points measured for RoCoF calculations (figure 4.8 and figure 4.9), these being test 3 and test 6. The results are found in Table 6.

Table 6 Calculated RoCoF performance

Test	Generator	Start Freq (Hz)	0.5 sec Freq (Hz)	1 sec Freq (Hz)	Event RoCoF (Hz/s)
3	Both	49.92	49.58	49.16	-0.76
6	freq1	49.84	49.19	48.32	-1.53

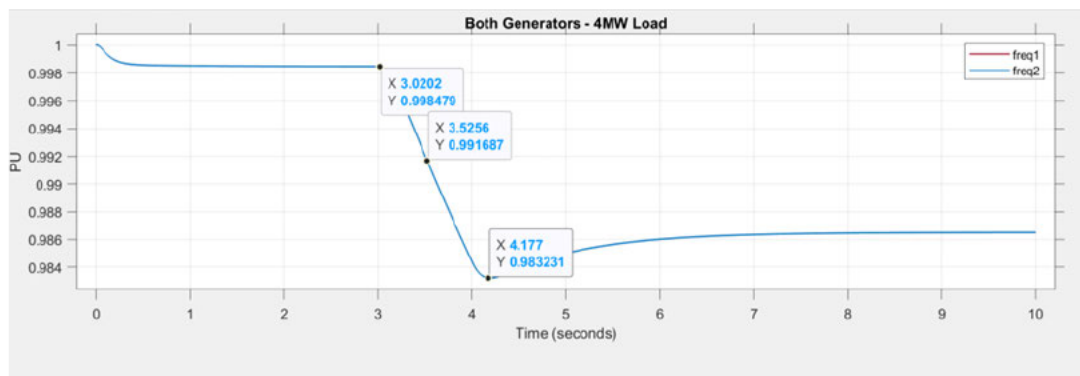


Figure 4.11 Test 3 data for RoCoF

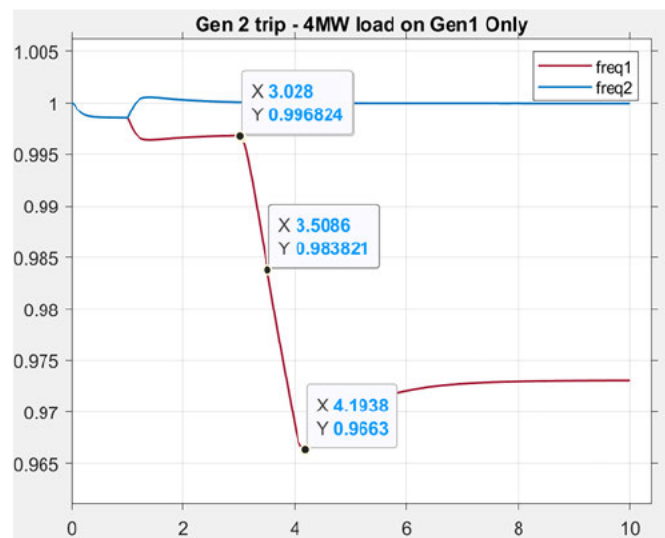


Figure 4.12 Test 6 data for RoCoF



The result for test 6 indicates it does not meet the 1Hz/s requirement for RoCoF, further if the frequency drops this far (48.32 Hz) it would potentially trigger an under-frequency load shed (UFLS) event.

4.2 FREQUENCY ASSESSMENT

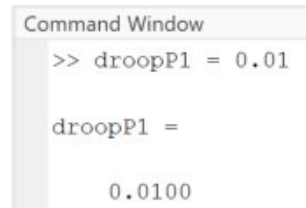
4.2.1 Overview

As part of the MATLAB code used for the various tests, two waveforms are generated as samples for all analysis, with each containing harmonic content. One waveform has a fundamental frequency, typically 50 Hz, and one harmonic frequency - 1042 Hz. The second waveform has one fundamental frequency and three harmonic frequencies – 150 Hz, 250 Hz and 1042 Hz. These harmonics were chosen as the first two, the 3rd and the 5th orders, are commonly seen on power networks and the last one is an example of an audio frequency load control (AFLC) signal, which is injected on power networks. The harmonic component amplitude was over exaggerated for demonstration and analysis purposes.

4.2.2 Generator Settings

The code establishes the droop settings for the model (figure 4.10). Using this method meant changing the droop values was a simple task of entering new values in the Command Window of MATLAB and then re-running the model (figure 4.11).

```
% Settings for simulink
droopQ1 = 0.05;
droopQ2 = 0.05;
droopP1 = 0.05;
droopP2 = 0.05;
```


Figure 4.13 Example code in MATLAB for model settings

```
Command Window
>> droopP1 = 0.01

droopP1 =

    0.0100
```

Figure 4.14. Example of adjusting settings via command window

4.2.3 Zero Crossing

The zero-crossing technique was calculated using the sample waveforms from the code. This technique involved the code finding a zero crossing, starting a timer, and then finding the next zero crossing. The time difference between the two would be equivalent to half of one cycle. In figure 4.12 as the system frequency approaches the zero crossing, the harmonic content is of such an amplitude that it crosses before the fundamental component. Further, there are multiple zero crossings in rapid succession around the time. This produces an erroneous indication of what the frequency as dependant on the sampling rate, each individual crossing would register. Table 7 displays the time measured between the zero crossings for the sample in figure 4.12, if the frequency was just a clean 50 Hz this would register as five crossings.

Few, if any, power systems are free of harmonic content therefore it is not a suitable technique for calculating the frequency from the voltage waveform.

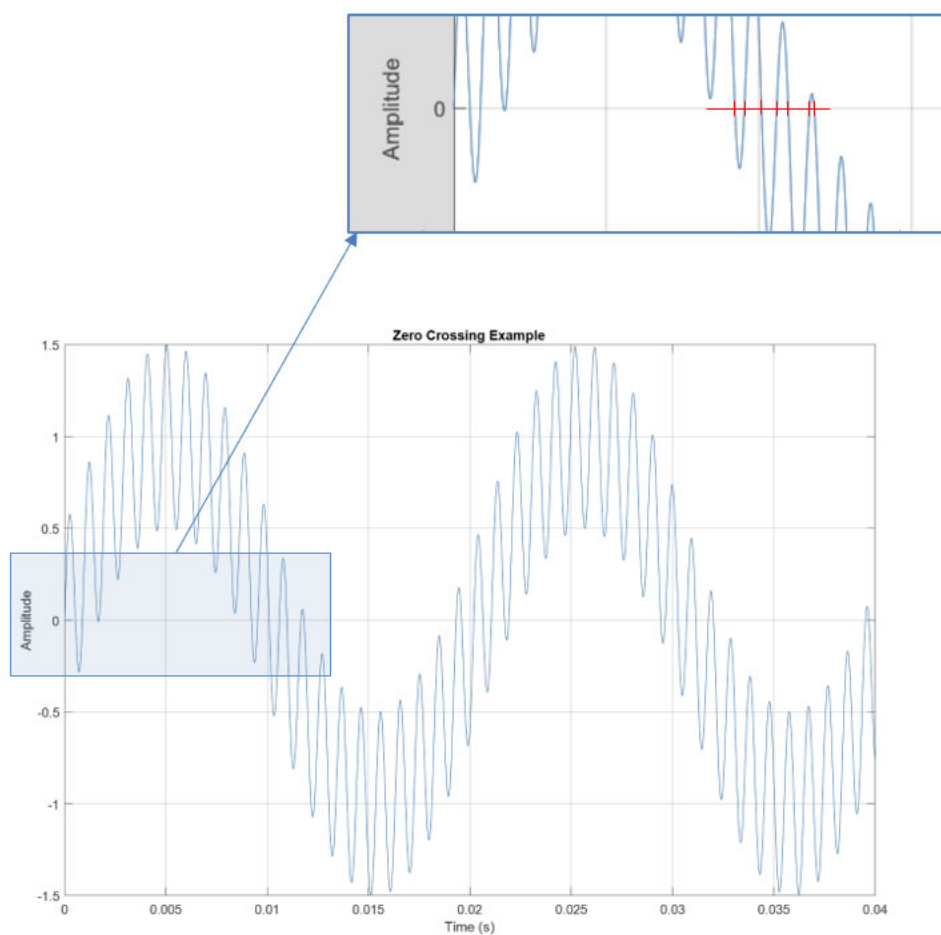


Figure 4.15. Zero crossing error - multiple zero crossings due to harmonic content

**Table 7 Results of zero crossing sample**

Time intervals between zero crossings milli- seconds
0.5
0.3
0.8
0.1
7.5
0.3
0.6
0.5
0.4
0.7
0.1
7.5
0.3
0.6
0.5
0.4
0.7
0.2
7.5
0.2
0.6
0.4
0.4
0.6
0.3
7.5
0.2
Number of zero crossings: 28

4.2.4. DFT

MATLAB has an inbuilt DFT tool which can be used for signal processing. This fundamentally applies a FFT for computing the DFT. The concept for the analysis of the frequency is to use this feature to identify the component frequencies that make up the distorted waveform. As the waveforms were generated with specific harmonics, it was simple to confirm the accuracy of the DFT.

4.2.4.1 Sampling Frequency

The sampling frequency is the rate at which the time signal is sampled when converting it to a discrete-time signal. The sample time was set to 3000 samples per second. This was chosen as it is above the Nyquist frequency ($2 \times 1042 = 2084$ Hz), which according to research should provide a result without any aliasing. Aliasing can cause the higher frequency to appear as lower distorted frequencies. The sampling period, the time intervals between samples, is the inverse of the sampling frequency (4.2):

$$Ts = \frac{1}{fs} \quad (4.2)$$

Where,

Ts – sampling time

fs – sampling frequency

So, for this code,

$$Ts = \frac{1}{3000} = 0.000333 \text{ seconds}$$



The code uses a five-second interval for the waveform generation, which was just an arbitrary value. The sample waveform containing four different frequencies is analysed using the DFT. For the actual analysis the code is simply:

```
Y = fft(xn, NFFT);
```

Where,

Xn - The sample waveform to be analysed,

NFFT – Number of points used in the FFT calculation

The amplitude and phase of each component of xn is calculated by the DFT, for every frequency bin, a corresponding discrete value for each frequency component, up to the Nyquist frequency. This provides a frequency domain representation of the waveform.

The frequency bin width is calculated based on the frequency resolution (4.3).

$$\Delta f = \frac{f_s}{NFFT} \quad (4.3)$$

So,

$$F_s = 3000 \text{ Hz}$$

$$NFFT = 1024$$

$$\Delta f = \frac{3000}{1024} = 2.93 \text{ Hz}$$

This calculation indicates that there is a 2.93 Hz spacing for each bin. Analyses of the bins involves finding the highest amplitude contained amongst them. This method identifies the dominant frequencies.

4.2.4.2 Peaks

Once the DFT has been calculated, the highest amplitude frequency components are identified. A filter is applied to narrow this down to between 48 – 50 Hz. These values were chosen as they will return the fundamental frequency component only, which is the objective of the analysis.

4.2.4.3 Results of DFT

For the first attempt at using the DFT the fundamental frequency of the sample waveform was altered as per Table 8. The resultant calculated frequency by the DFT can be observed in column two of Table 8.

Table 8 Initial DFT results

Fundamental frequency of generated waveform (Hz)	DFT calculated fundamental frequency (Hz)
48.25	48.8
48.5	48.4
48.75	48.2
49	49
49.25	49.2
49.5	49.4
50	50

As can be seen from Table 2, the fundamental frequency calculated by the DFT had a considerable deviation from that generated in the sample code making it unsuitable in its current form, as the frequency operating standards stipulate an accuracy to two decimal places.

4.2.4.4 DFT Accuracy

The accuracy of the DFT could be improved by increasing the value of NFFT. This would increase the frequency resolution, better distinguishing closely spaced frequency components, however, this would have an offset of increased computational effort and efficiency.

Another method to improve the accuracy of the result is to use zero padding. Zero padding adds additional zeros to the end of the frequency signal (x_n – in the code) to increase its length while not actually changing its value. This effectively increases the number of points analysed in the FFT and thereby creates more frequency bins i.e., a better definition of the frequency components.

With zero padding the NFFT is much greater than the number of samples (N – in the code) based on the sampling rate, 3000 samples/ sec for 5 seconds.

$$N = 5 \times 3000 = 15000$$

If NFFT was set to equal N the frequency resolution would be, using (4.3):

$$\Delta f = \frac{3000}{15000} = 0.2 \text{ Hz}$$

This value yielded the results found in the initial operation of the DFT, see Table 2.

Applying zero padding, commonly a power of two greater than the value of N , speeds up the FFT calculation. For the code a value of 10 times was chosen arbitrarily, this gave a NFFT of:

$$N \times 10 = 15000 \times 10 = 150000$$

Using MATLAB, the next power of two greater than this is

$$2^{18} = 262144$$

So, the NFFT is set to 262144 and the frequency resolution becomes

$$\Delta f = \frac{3000}{262144} = 0.0572 \text{ Hz}$$

This is a much finer bin value and should return an accurate fundamental frequency.

4.2.4.5 Results of Zero Padding

The same series of fundamental frequencies in Table 2 were tested again with the adjusted number of sampling points (NFFT). The results can be observed in Table 9.

Table 9 Fundamental frequency comparison

Fundamental frequency of generated waveform (Hz)	DFT calculated fundamental frequency (Hz)
48.25	48.25
48.5	48.5
48.75	48.75
49	49
49.25	49.25
49.5	49.5
50	50
51.11	51.11

By applying the zero-padding technique the code returned an exact match, accurate to better than two decimal places, and meeting the criteria of the network frequency standards.

A display was developed for testing that showed the original distorted waveform, the Fourier bin values/ component frequency amplitudes and the reconstructed fundamental component frequency (figures 4.13 and 4.14). in figure 4.14 the fundamental frequency in the sample waveform was set to 51.11 Hz, this can be observed in the reconstructed waveform.

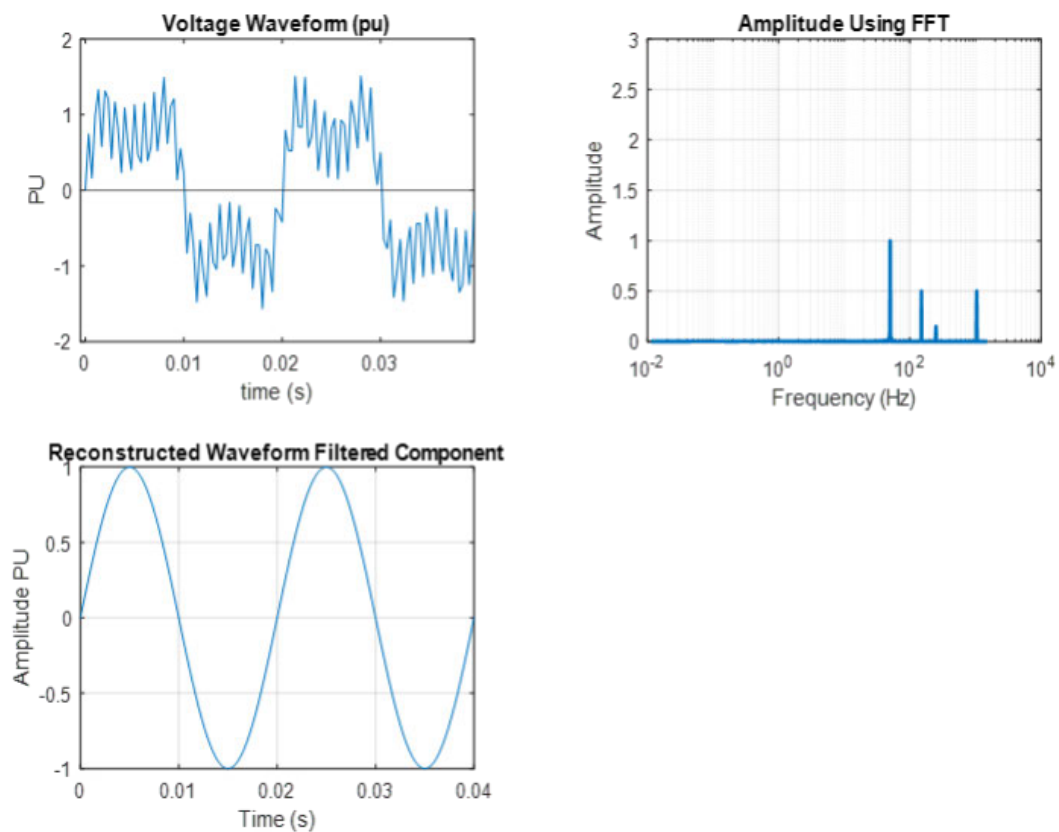


Figure 4.16 DFT process display – 50 Hz fundamental

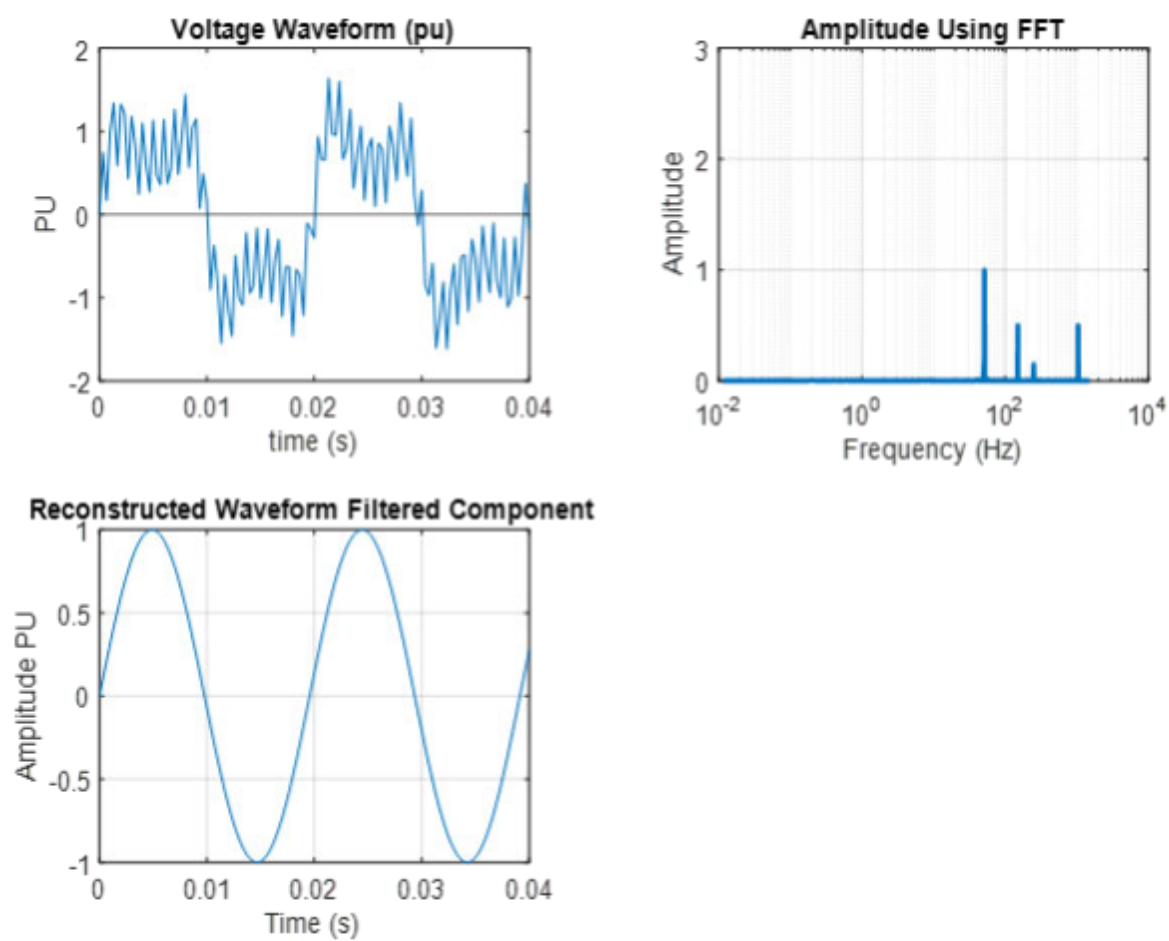


Figure 4.17. DFT process display - 51.11 Hz fundamental

4.2.5 ROCOF

To prove the method of calculating RoCoF an example event found in the literature review, the South Australian state-wide outage, was modelled.

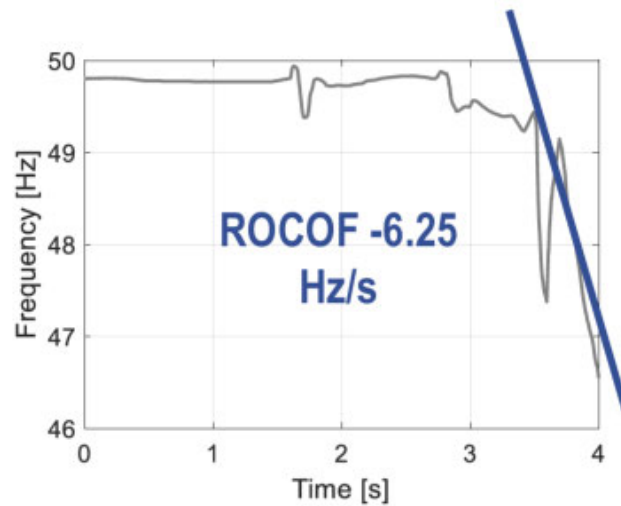


Figure 4.18 South Australia state outage

Data points were reproduced as accurately as possible from the graph in Figure 4.13. A new MATLAB code was developed, and the data points were entered. This was then analysed and returned a RoCoF value for this event of -5.65 . This is reasonably accurate as the actual raw data was not available for the event and the points were estimated from the diagram. The code also interpolated the data to determine the frequency profile. The reproduced frequency profile from the MATLAB result for the last 1.8 seconds of the event can be seen in Figure 4.14.

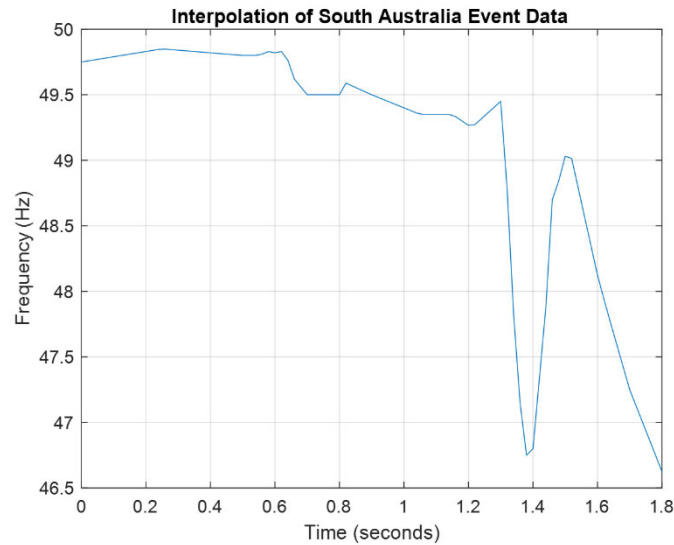


Figure 4.19 Reproduced frequency profile for SA event (last 1.8 seconds only)

4.2.6 Sliding DFT

The results have established that a DFT is a fast and accurate method of determining the fundamental frequency of a distorted voltage waveform.

To apply this in a real time environment a new sliding DFT (SDFT) code was developed based on the modelling so far. The new model is run for 10 seconds as an example.

Initial modelling of a SDFT has a code that uses a randomly generated waveform with frequency variations centred around 50 Hz, as such the sampling frequency is set to 1000 samples per second for improved efficiency which produced 20 samples per cycle.

As a part of the development of this code an ‘event capture’ feature was developed which applied RoCoF calculations to any frequency excursions. For the simulation, the code



generates random RoCoF event/s with a duration of 0.5 seconds or more, to ensure they exceed the limits in the standards.

For the analysis of the sampling frequency, a 0.5 second window is 'sliding' in 0.01 second increments i.e., half cycle sampling for 50 Hz. The concept is that it will capture multiple cycles of the frequency for analysis. At 0.5 seconds and with the sampling frequency set to 1000 it means there will be 500 samples per sliding window.

Two thresholds are established as part of the initialisation of the code. One for frequency excursion with the limit set to ± 0.5 Hz based on the normal operating band found in the frequency operating standards. The other threshold is RoCoF which is set to ± 1 Hz, which will be time waited over one second, but calculated in 0.5 second increments.

A loop is established to generate the random RoCoF event times. The results of this are then summated using a cumulative sum which incorporates the frequency fluctuations with a baseline 50Hz signal, thereby generating a random frequency with RoCoF characteristics.

Several different matrixes and structures are established in the code and set with zeros where applicable. A loop is set to monitor the frequency during the SDFT process. Again, zero padding was employed to improve the accuracy and quality of the SDFT result.

Once run a peak detection locates the peak frequency and stores the result. The resulting value is assessed and if outside the threshold it will record an excursion. The RoCoF is

calculated by comparing the frequency to the previous 500ms value and triggering if outside the RoCoF threshold, figure 4.15 displays the result using the SDFT code. An example system alarm is generated to alert an operator of a frequency excursion and RoCoF event, figure 4.16.

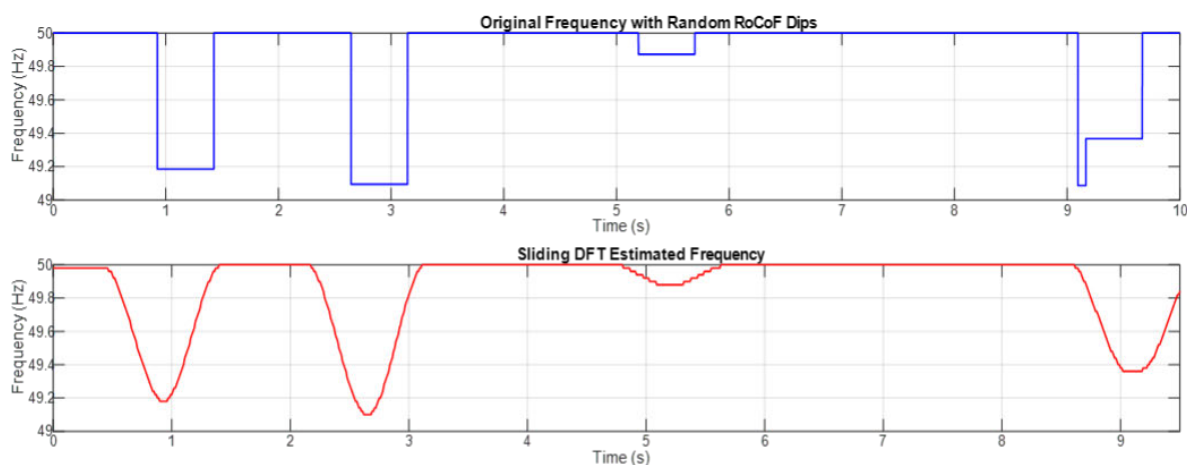


Figure 4.20. Result of SDFT versus sample frequency

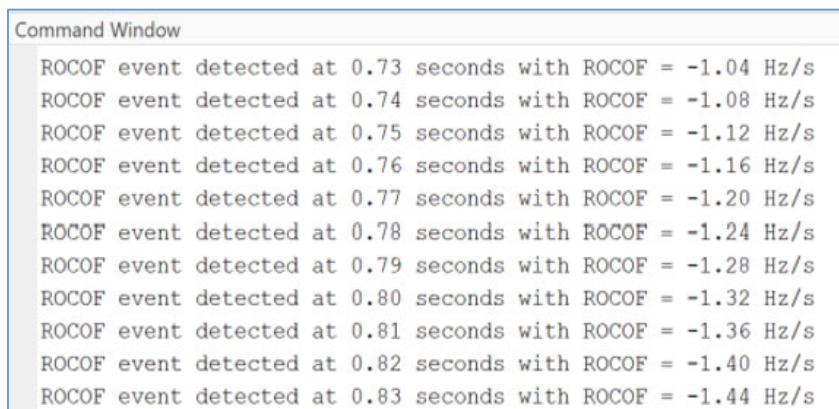


Figure 4.21 Example system operator RoCoF alert



4.2.7 CHAPTER SUMMARY

In respect to objective 4, a model was developed that could display the frequency, as an indication of inertia, in real time. The modelling unfortunately did not work as one complete system, however, works in fragmented sections. The final code (SDFT) uses simulated waveforms and generates events when excursions occur.

When combined the results reflect the methodology in that a distorted voltage waveform is filtered, the frequency determined and any RoCoF event is registered.



CHAPTER 5 CONCLUSIONS

The main objective of this dissertation was to devise a method of assessing power system inertia in real time. Research has revealed there is a concerning and emerging problem worldwide as renewable energy resources are displacing synchronous generation, as there is uncertainty if renewable energy can provide equivalent levels of inertia. Differing forms of renewable resources can produce synthetic inertia, where the power electronic interface between the source and the grid mimics the inertia of a synchronous generator. This synthetic inertial response is not a fixed constant, rather it's a controlled response where alternate parameters can be applied between different technologies. While synthetic inertial response is theoretically capable, there exists no standard for its implementation yet.

Assessing the power system frequency is an accepted industry approach to evaluating the system inertia, as the system frequency is directly related to the angular velocity of the rotor in a synchronous generator. The mass of this large rotor provides the system with inertia.

Initially methods of measuring the system frequency used a technique of timing the zero crossing points of a voltage waveform. This proved to be unsuccessful when heavily distorted waveforms were assessed as erroneous extra crossing were captured.

The final technique, that delivered the main objective of the project, used a sliding discrete Fourier transform to analyse the frequency of the voltage waveform. This transform separates the waveform into component frequencies, which then can be filtered to return just the desired fundamental frequency. A sliding window performs a discrete transform every 500ms and compares this to the next 10ms of the waveform continuously. The result is



assessed against predefined criteria, with any excursions assessed against RoCoF criteria and a message is generated alerting a system operator a RoCoF event has occurred.

FURTHER WORK

A method was developed for assessing the inertia in a power system; however, several opportunities are present to improve on the solution presented and provide a more rigorous product. These include:

- 1) Incorporate the filtering into the sliding DFT. Due to limitations of coding skills the code was fragmented and was operated in sperate sections. Further development would combine this into one code.
- 2) Further development of the model to include the more complex power electronic interface of renewable energy, including synthetic inertia modelling.
- 3) Have the system run based on the Simulink model frequency. Incorporate the sliding DFT with the Simulink model, and have the model run a distorted waveform.
- 4) Expand experimentation to use real world voltage waveform via a suitable transducer. The waveform used could simply be a local LV supply i.e. a 240v general purpose outlet.



CHAPTER 6 REFERENCE LIST

AEMC n.d., *A.1 Frequency operating standards for the mainland NEM A.1.1 Part A Summary of the Frequency operating standards for the mainland NEM*, viewed 1 September 2023, <<https://www.aemc.gov.au/sites/default/files/content/c2716a96-e099-441d-9e46-8ac05d36f5a7/REL0065-The-Frequency-Operating-Standard-stage-one-final-for-publi.pdf>>.

AEMO 2020a, *Power System Requirements*, www.aemo.com.au, AEMO, viewed 2 November 2023, <https://www.aemo.com.au/-/media/Files/Electricity/NEM/Security_and_Reliability/Power-system-requirements.pdf>.

— 2020b, *System Strength System strength in the NEM explained*, Australian Energy Market Operator, March, AEMO, viewed September 2023, <<https://aemo.com.au/-/media/files/electricity/nem/system-strength-explained.pdf>>.

— 2021, *Application of Advanced Grid-scale Inverters in the NEM White Paper An Engineering Framework report on design capabilities needed for the future National Electricity Market*, AEMO, viewed 2 November 2023, <<https://aemo.com.au/-/media/files/initiatives/engineering-framework/2021/application-of-advanced-grid-scale-inverters-in-the-nem.pdf>>.

AEMO, A 2020c, *Renewable Integration Study: Stage 1 report Enabling secure operation of the NEM with very high penetrations of renewable energy*, viewed 2 August 2024, <<https://aemo.com.au/-/media/files/major-publications/ris/2020/renewable-integration-study-stage-1.pdf>>.

— 2023, *Inertia in the NEM explained*, Australian Energy Market Operator, March, AEMO, viewed September 2023, <<https://aemo.com.au/-/media/files/initiatives/engineering-framework/2023/inertia-in-the-nem-explained.pdf?la=en>>.

AEMO & AEMC 2022, *Essential system services and inertia in the NEM*, Australian Energy Market Operator, June, AEMO, viewed September 2023, <<https://www.aemc.gov.au/sites/default/files/2022-06/Essential%20system%20services%20and%20inertia%20in%20the%20NEM.pdf>>.

babu, phani 2022, *What is Generator Capability Curve?*, ELECTRICAL ENGINEERING MATERIALS, viewed 2 March 2024, <<https://electengmaterials.com/what-is-generator-capability-curve/>>.

Chown, G, Wright, J, Van Heerden, R & Coker, M 2017, *Cigré 2017 8th Southern Africa Regional Conference System inertia and Rate of Change of Frequency (RoCoF) with increasing non- synchronous renewable energy penetration **Energy System Planning (ESP) (South Africa)*, CIGRE.

Denholm, P, Mai, T, Kenyon, R, Kroposki, B & O'malley, M 2020, *Inertia and the Power Grid: A Guide Without the Spin*, viewed 1 September 2023, <<https://www.nrel.gov/docs/fy20osti/73856.pdf>>.

entsoe 2020, *Inertia and Rate of Change of Frequency (RoCoF)*, <https://eepublicdownloads.entsoe.eu/>, ENTSOE, p. 48, viewed 2 October 2023, <https://eepublicdownloads.entsoe.eu/clean-documents/SOC%20documents/Inertia%20and%20RoCoF_v17_clean.pdf>.

Grainger, J & Stevenson, WD 1994, *Power System Analysis*, McGraw-Hill Companies.

Hou, Y, Xu, J, Wang, J & Wu, X 2019, 'A Review on Dynamic Analysis Methods of Power System Frequency', *A Review on Dynamic Analysis Methods of Power System Frequency*.

Iain Explains Signals and Systems 2019, *How do Complex Numbers relate to Real Signals?*, YouTube, viewed 31 October 2020, <<https://www.youtube.com/watch?v=TLWE388JWGg>>.

Iain Explains Signals, Systems, and Digital Comms 2019, *Fourier Transform Equation Explained* ('Best explanation of the Fourier Transform on all of YouTube'), YouTube, viewed 2 November 2024, <<https://www.youtube.com/watch?v=8V6HikP9EE&list=PLx7-Q20A1VYJVLBCkuOBoBnaUdd5Qyms&index=4>>.

Nam, S-R, Kang, S-H & Kang, S-H 2014, 'Real-Time Estimation of Power System Frequency Using a Three-Level Discrete Fourier Transform Method', *Energies*, vol. 8, no. 1, pp. 79–93.

Quito, B, del Río-Rama, M de la C, Álvarez-García, J & Durán-Sánchez, A 2022a, 'Impacts of industrialization, renewable energy and urbanization on the global ecological footprint: A quantile regression approach', *Business Strategy and the Environment*, vol. 7.

— 2022b, 'Impacts of industrialization, renewable energy and urbanization on the global ecological footprint: A quantile regression approach', *Business Strategy and the Environment*, vol. 7.

Seeber, R & Ulrici, A 2016, 'Analog and digital worlds: Part 1. Signal sampling and Fourier Transform', *ChemTexts*, vol. 2, no. 4.

Serov, AN, Ivanenko, KA & Serov, NA 2021, 'Application of Sliding DFT Filtration to Improve Frequency Measurement Accuracy of Zero Crossing Technique', *Application of Sliding DFT Filtration to Improve Frequency Measurement Accuracy of Zero Crossing Technique*.

Simulink Instructor 2022, *Matlab Scripting for Simulink*, YouTube, viewed 2 November 2024, <<https://www.youtube.com/watch?v=qmlUjwWIZIE>>.

Tielens, P & Van Hertem, D 2016, 'The relevance of inertia in power systems', *Renewable and Sustainable Energy Reviews*, vol. 55, pp. 999–1009.



VisibleBreadcrumbs 2024, Mathworks.com, viewed 2 July 2024,
<<https://au.mathworks.com/help/sps/ref/powersystemssimulationonramp.html>>.

WU, Z, GAO, W, GAO, T, YAN, W, ZHANG, H, YAN, S & WANG, X 2017, 'State-of-the-art review on frequency response of wind power plants in power systems', *Journal of Modern Power Systems and Clean Energy*, vol. 6, no. 1, pp. 1–16.

Xu, T, jANG, W & Overbye, T 2018, 'Location-Dependent Impacts of Resource Inertia on Power System Oscillations', *Location-Dependent Impacts of Resource Inertia on Power System Oscillations*, vol. 1, no. 1, p. 6.



APPENDIX A SPECIFICATION

Specification and Work Plan

Title: Dynamic Assessment of System Inertia in Emerging Transmission Networks in Real Time

Name : Brad Christopher

Student ID : 

Supervisor: Dr Yi Cui

Introduction and Background

The objective of this research is to develop an innovative real-time power system inertia estimation tool that give Transmission and Network Providers (TNSPs) the ability to gauge their system security. Power system inertia is the aggregate equivalent inertia of all devices on the power system capable of providing inertial response, which is the initial, instant electrical power transfer from an apparatus in response to a disturbance in the system frequency. The system frequency must be strictly maintained within rigid constraints to avoid loss of both generation and loads and is a key part of system security.

Both (AEMO) and (Denholm et al. 2020) acknowledge the traditional formation of a power system using synchronous generation, stating the networks are connected to many large synchronous generators synchronised together I.e., in lock step. The machines revolve at high speed and thus rotational kinetic energy is stored in their mass which provides an electromechanical inertia which is then electro-magnetically coupled to the power system frequency I.e., in Australia 50 Hz. This kinetic energy can provide an inertial response, an immediate electrical power transfer from the generator to the network, when a frequency



disturbance occurs, which then attempts to maintain the frequency through any power system disturbance. Adequate Power system inertia is directly associated with maintaining the power system frequency. As an example, it is a requirement that the frequency in Australia is to be kept in the range of 49.85 Hz and 50.15 Hz (AEMC). Power system frequency is the inverse of the number of full rotations of a generator per second and is a critical parameter in maintaining the balance between generation and consumption of electricity (Zografos, Ghandhari & Eriksson 2018 & AEMO).

In recent years there has been a rise in the introduction of renewable energy source (RES) connected to the network which are displacing the traditional synchronous generators. RESs are unable to provide the same inertia as that of a synchronous generator as they use electronic converter-interfaces or inverter-based resource (IBR) to connect to the network and this is expected to reduce the overall system inertia. Due to the intermittent nature of RESs, the overall inertia of modern power systems will vary significantly during the day, resulting in frequency stability issues. (Kontis et al. 2021). (Zografos, Ghandhari & Eriksson 2018 & AEMO) further re-enforce the requirement to understand that synchronous generation is reducing whilst virtual inertia via IBR is increases will have an impact on the overall network inertia.

Modern RES does have the ability to mimic the characteristic of a synchronous generator and can provide virtual or synthetic inertia to overcome inertia shortfall due to the phasing out of synchronous generators. However, the introduction of a large amount of variable inertia changes the inertia distribution of the original system and interacts with damping characteristics, and unreasonable parameters even risk the instability of the system oscillation (Peng et al. 2023).



Objectives and Aims

The aim of the project will be the development of inertia tool which can generate ‘heatmap’ type imagery to highlight any problematic areas of a transmission network. Further the inertia tool will be capable of modelling the system inertia for future network augmentations.

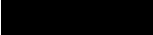
Specific Objectives:

- **Research** - Provide relevant evidence that addresses the theoretical problem identified. Provide a practical solution to address the theoretical problem.
- **Model Development** - Using industry accepted programs produce a suitable network model that realistically mimics an actual network upon which simulations of disturbances can occur.
- **Data Collection** - Obtain real data from a known event to test network model
- **Inertia Tool Development** - I Develop a tool that can display the system inertia in real time

Expected Outcomes:

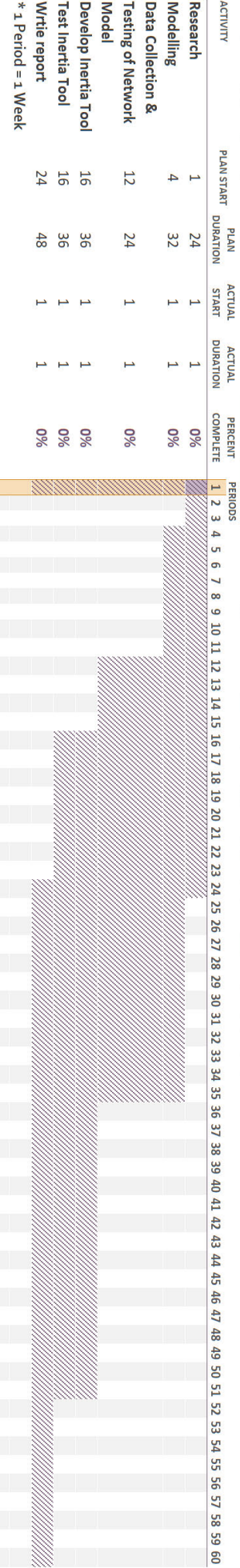
The outcomes expected of this proposal are:

1. An improved understanding of system inertia for TNSPs in general and network operators
2. Improved visibility of the state of the power system inertia in real time
3. TNSPs will be better equipped to respond to network disturbances and can respond to potential network security shortfalls before they cause outage



Research Project

Select a period to highlight at right. A legend describing the charting follows.



Work Plan

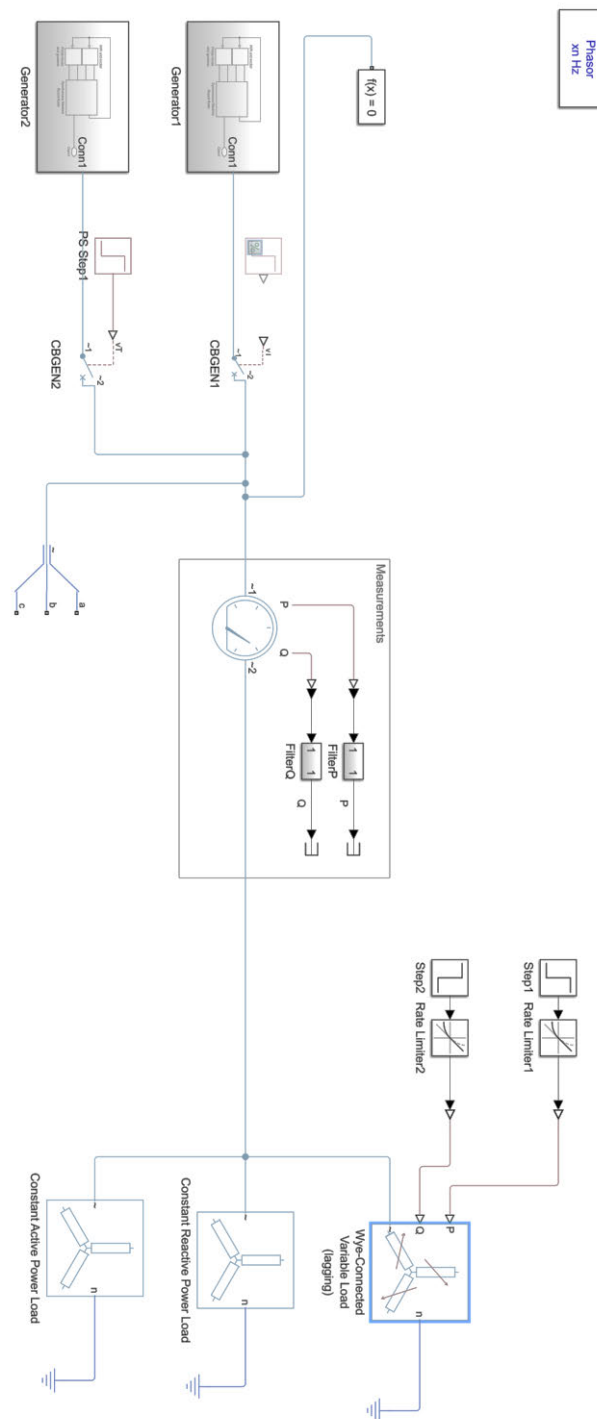


Resources Required:

The resources required are expected to be minimal. Data collection will be via remote connection to relays and power quality monitoring. Other data sources could be via communication with other utilities etc.

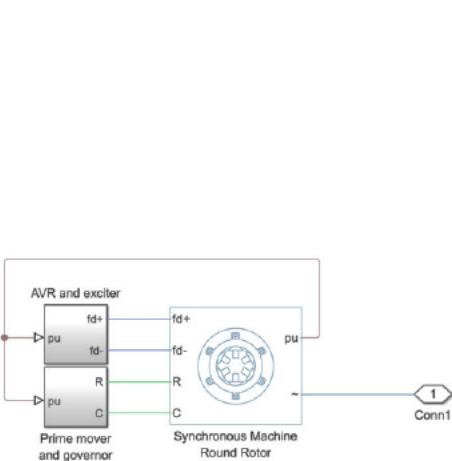
Specific Software requirements include MATLAB, PowerFactory and PSCAD. Other software will include standard Microsoft suite – Word, Excel, etc.

The following details the settings used for the key components in the network model in Simulink



Round rotor synchronous generator

Settings	Description	VALUE
NAME		VALUE
Modeling option		No thermal port
Main		
Electrical connection		Composite three-phase ports
> Rated apparent power	5e6	A*V
> Rated voltage	4160	V
> Rated electrical frequency	50	Hz
> Number of pole pairs	4	
Specify parameterization by		Standard parameters
Specify field circuit input required to prod...		Field circuit current
> Field circuit current	50	A
Zero sequence		Exclude
Rotor angle definition		Angle between the a-phase magnetic axis and the d-axis
Impedances		
> Stator resistance, Ra	0.003	
> Stator leakage reactance, Xl	0.15	
> d-axis synchronous reactance, Xd	1.81	
> q-axis synchronous reactance, Xq	1.76	
> d-axis transient reactance, Xd'	0.3	
> q-axis transient reactance, Xq'	0.65	
> d-axis subtransient reactance, Xd''	0.23	
> q-axis subtransient reactance, Xq''	0.25	
Time Constants		
Specify d-axis time constant		Open circuit
> d-axis transient open-circuit, Td0'	5.25	s
> d-axis subtransient open-circuit, Td0''	0.03	s
Specify q-axis time constant		Open circuit
> q-axis transient open-circuit, Tq0'	1	s
> q-axis subtransient open-circuit, Tq0''	.07	0.07 s
Saturation		
Magnetic saturation representation		None
Initial Conditions		
Initialization option		Set real power, reactive power, terminal voltage, and termin
> Terminal voltage magnitude	4160	V
> Terminal voltage angle	0	deg
> Active power generated	2e3	A*V
> Reactive power generated	0	A*V



AVR & Exciter

Synchronous machine field circuit

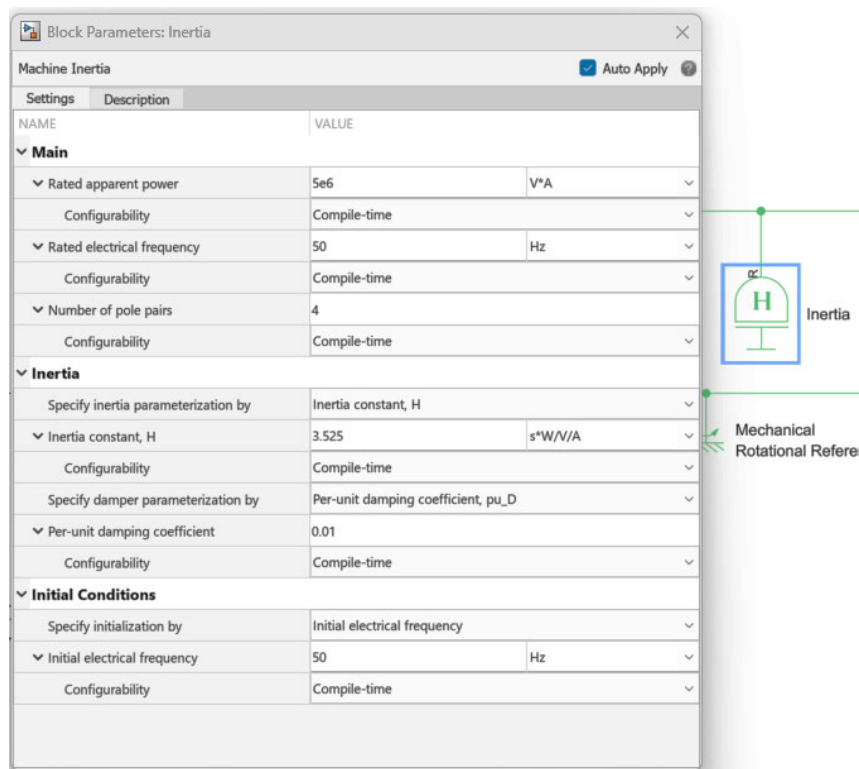
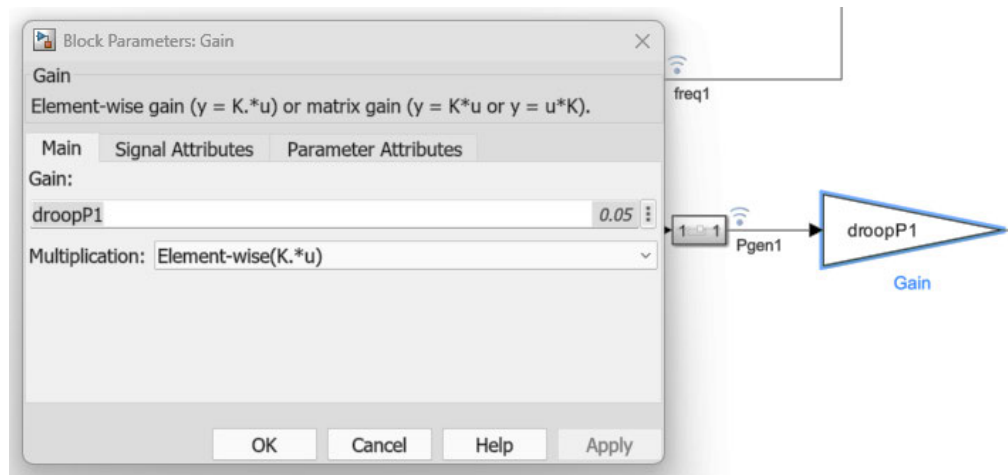
Block Parameters: Synchronous Machine Field Circuit (pu)

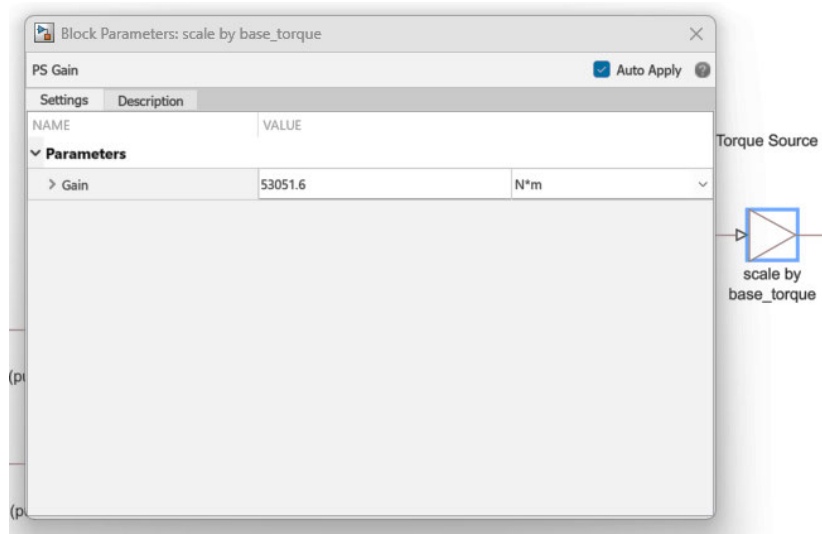
Synchronous Machine Field Circuit ☒ Auto Apply

Settings	Description	VALUE
▼ Main		
PS input and output unit	Per unit	▼
▼ Rated apparent power	5e6	V*A ▼
Configurability	Compile-time	▼
▼ Rated electrical frequency	50	Hz ▼
Configurability	Compile-time	▼
Specify field circuit input required to prod...	Field circuit current	▼
▼ Field circuit current	50	A ▼
Configurability	Compile-time	▼
▼ Machine Parameters		
Specify parameterization by	Standard parameters	▼
> Stator leakage reactance, X_l	0.15	
> d-axis synchronous reactance, X_d	1.05	
> d-axis transient reactance, X_d'	0.35	
> d-axis subtransient reactance, X_d''	0.23	
Specify d-axis time constant	Open circuit	▼
> d-axis transient open-circuit, T_{d0}'	5.25	s ▼
> d-axis subtransient open-circuit, T_{d0}''	0.03	s ▼

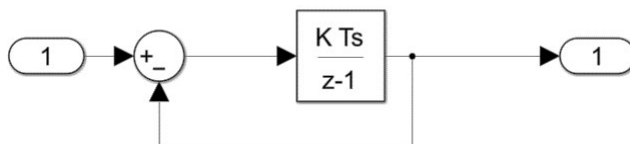
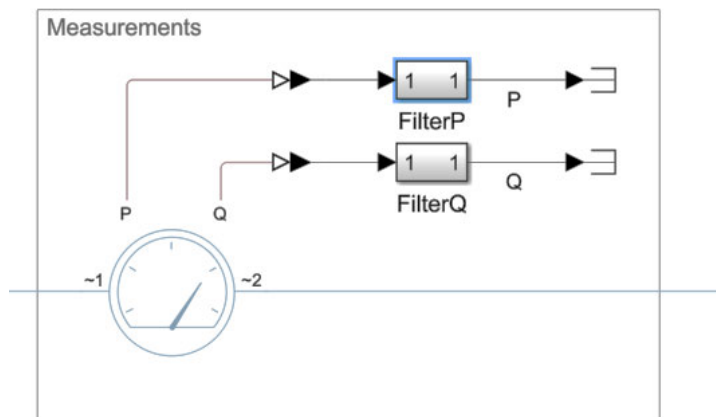
Synchronous Machine Field Circuit (pu)

The diagram shows a block representing the Synchronous Machine Field Circuit (pu). It has two inputs: E_{fd_pu} (positive terminal) and I_{fd_pu} (negative terminal). The output is labeled $fd+$ and $fd-$.

Prime Mover & Governor

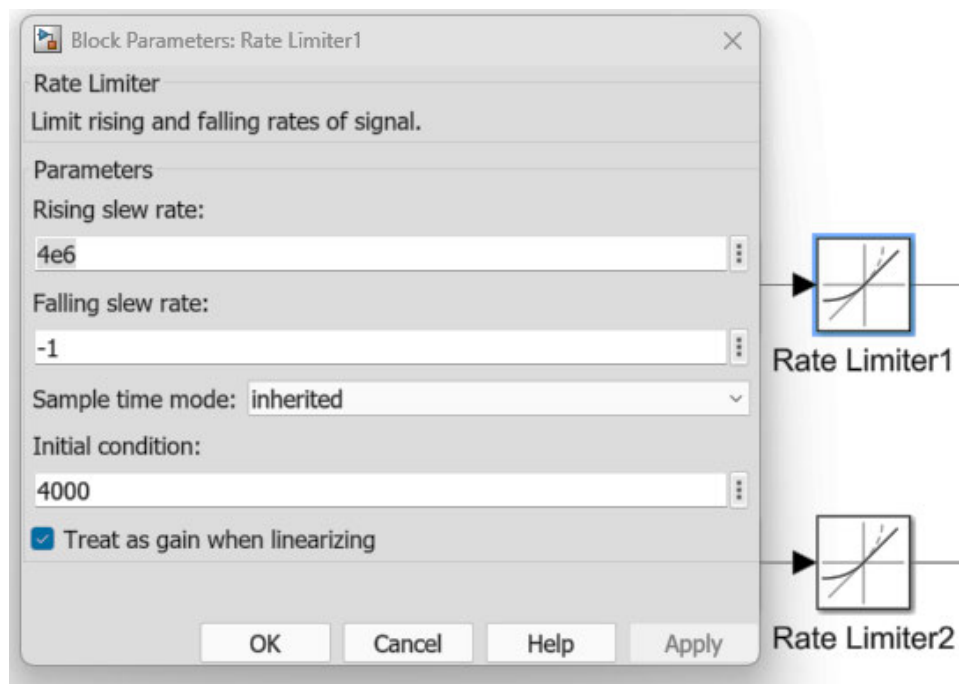
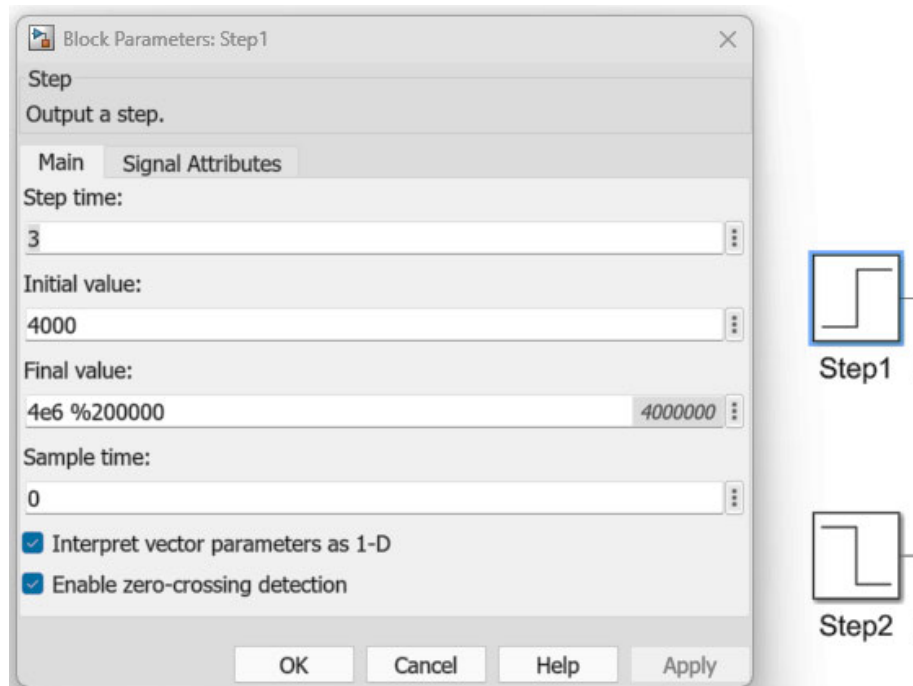


Measurement block



P & Q filters are both the same

Load control





Loads

Block Parameters: Constant Reactive Power Load

Wye-Connected Load

Settings

Description

NAME

VALUE

Modeling option

Composite three-phase ports

Main

Parameterization

Specify by rated power

Component structure

L

Rated voltage

4160*0.98

4076.8 V

Configurability

Compile-time

Rated electrical frequency

50

Hz

Configurability

Compile-time

Inductive reactive power

6000

A*V

Configurability

Compile-time

Parasitics

Parasitic parallel conductance

0

1/Ohm

Initial Conditions

Terminal voltage magnitude

4160*0.98

4076.8 V

Terminal voltage angle

0

deg

Frequency

50

Hz

P

Q

n

Wye-Connected Variable Load (lagging)

n

Constant Reactive Power L

n

Constant Active Power Load

Block Parameters: Constant Active Power Load

Wye-Connected Load

Settings

Description

NAME

VALUE

Modeling option

Composite three-phase ports

Main

Parameterization

Specify by rated power

Component structure

R

Rated voltage

4160

V

Configurability

Compile-time

Real power

500e3

W

Configurability

Compile-time

n

Constant Reactive Power Load

n

Constant Active Power Load



Block Parameters: Wye-Connected Variable Load (lagging)

Wye-Connected Variable Load (lagging)

Auto Apply

Settings	Description	VALUE
NAME		
Modeling option		Composite three-phase ports
Main		
Rated voltage	4160	V
Configurability		Compile-time
Rated electrical frequency	50	Hz
Configurability		Compile-time
Minimum real power	1e3	W
Configurability		Compile-time
Minimum reactive power	100	A*V
Configurability		Compile-time
Parasitics		
Parasitic parallel conductance	1e-6	1/Ohm
Initial Targets		
<input type="checkbox"/> Three-phase currents		
<input type="checkbox"/> Three-phase magnetic fluxes		
Nominal Values		
<input type="checkbox"/> Three-phase currents		
<input type="checkbox"/> Three-phase magnetic fluxes		

P

Q

n

Wye-Connected Variable Load (lagging)

n

Constant Reactive Power Load

Salient Pole Generator

Synchronous Machine Salient Pole Auto Apply

Settings	Description	VALUE	
NAME			
▼ Rated apparent power		5e6	A*V
Configurability		Compile-time	
▼ Rated voltage		4160	V
Configurability		Compile-time	
▼ Rated electrical frequency		50	Hz
Configurability		Compile-time	
▼ Number of pole pairs		4	
Configurability		Compile-time	
Specify parameterization by		Standard parameters	
Specify field circuit input required to prod...		Field circuit current	
▼ Field circuit current		50	A
Configurability		Compile-time	
Zero sequence		Exclude	
Rotor angle definition		Angle between the a-phase magnetic axis and the d-axis	
▼ Impedances			
▼ Stator resistance, Ra		0.011	
Configurability		Compile-time	
> Stator leakage reactance, Xl		0.15	
> d-axis synchronous reactance, Xd		1.05	
> q-axis synchronous reactance, Xq		0.7	
> d-axis transient reactance, Xd'		0.35	
> d-axis subtransient reactance, Xd''		0.25	
> q-axis subtransient reactance, Xq''		0.325	
▼ Time Constants			
Specify d-axis time constant		Open circuit	
> d-axis transient open-circuit, Td0'		5.25	s
> d-axis subtransient open-circuit, Td0''		0.03	s
Specify q-axis time constant		Open circuit	
> q-axis subtransient open-circuit, Tq0''		0.05	s
▼ Saturation			
Magnetic saturation representation		None	
▼ Initial Conditions			
Initialization option		Set real power, reactive power, terminal voltage, and termi	
> Terminal voltage magnitude		4160	V
> Terminal voltage angle		0	deg
> Active power generated		2e3	A*V
> Reactive power generated		0	A*V

Variant Subsystem

Subsy Refer

COMI

Salient Pole Generator
5MVA

108%

80%



APPENDIX C MATLAB CODE

The following is the codes used for this dissertation. I have not edited mistakes etc as they are a direct copy out of MATLAB.

Plot waveform and DFT

```
%%%%%%%%%%%%%%%%%%%%%%%%%%%%%%%%%%%%%%%%%%%%%%%%%%%%%%%%%%%%%%%%%%%%%%%%
% Code creates one of two sample waveforms, performs DFT and reconstructs
% the fundametal waveform based on limits set in the code.
%%%%%%%%%%%%%%%%%%%%%%%%%%%%%%%%%%%%%%%%%%%%%%%%%%%%%%%%%%%%%%%%%%%%%%%%
% author: Brad Christopher with assistance from Mathworks onramp training, online resources &
% searches
```

```
clear
clc
% Settings for simulink
droopQ1 = 0.05;
droopQ2 = 0.05;
droopP1 = 0.05;
droopP2 = 0.05;
fs = 3000; % samples per second
t = 0:1/fs:5-1/fs; % time vector for 1 second duration - changed to 5
A = 1; % set to 1 pu
% Create sample waveform with Harmonics
x1 = A*sin(2*pi*50*t);
x2 = (0.5*A)*sin(2*pi*150*t);
x3 = (0.15*A)*sin(2*pi*250*t);
x4 = (0.5*A)*sin(2*pi*1042*t);
xn = x1 + x2 + x3 + x4; % Select desired distortion - line 31 or 32
%xn = x1 + x4;
N = length(xn); % Number of samples

%% Determine Fundamental frequency %%
% First round of DFT had no zero padding - for demonstration kept this in
% the code, do not use line 42
% NFFT = N;% Comment out for final version - just here for intial round
% Moderate zero-padding to increase frequency resolution
NFFT = 2^nextpow2(N*10); % 10 Moderate increase in FFT length ...
% to improve accuracy of final calc

Y = fft(xn, NFFT); % Performs DFT
% Split into One-sided amplitude spectrum
xk = abs(Y)/N;
xk = xk(1:NFFT/2+1); % One sided removes negative samples
xk(2:end-1) = 2*xk(2:end-1); % Doubles values except for DC (1st) and ...
% Nyquist (last) results
% Corrected frequency vector
```



```
fr = (0:(NFFT/2))*(fs/NFFT);
% Find the peak frequencies
[pks, locs] = findpeaks(xk, 'MinPeakHeight', 0.5); % Lower 'MinPeakHeight' to capture peaks - set
only as high as req'd
pkFreq = fr(locs);
% Filter frequencies within the desired range
filt_freq = pkFreq(pkFreq >= 48 & pkFreq <= 52);
Fund_freq = A*sin(2*pi*filt_freq*t);
%% Display the filtered frequency with two decimal places
disp('Filtered freq:');
fprintf('%0.2f Hz\n', filt_freq);

%% plots of results
% for visual understanding only

% Initial distorted waveform
figure;
nexttile
plot(t,xn)
yline(0);
xlabel('time (s)');
title('Voltage Waveform (pu)');
xlim([0 0.04])
hold on
% DFT
nexttile
semilogx(fr, xk, 'LineWidth', 2)
ylim([0 3])
grid on
title ('Amplitude Using FFT')
xlabel('Frequency (Hz)')
ylabel('Amplitude')
% Re-constructed waveform
nexttile
plot(t, Fund_freq);
xlim([0 0.04])
title('Reconstructed Waveform Filtered Component');
xlabel('Time (s)');
ylabel('Amplitude');
grid on;
```



Zero crossing count

This code used the same waveform generation as the first code.

```

%%%%%%%%%%%%%%%%%%%%%%%%%%%%%%%%%%%%%%%%%%%%%%%%%%%%%%%%%%%%%%%%%%%%%%%%
%%%%%%%%%%%%%%%%%%%%%%%%%%%%%%%%%%%%%%%%%%%%%%%%%%%%%%%%%%%%%%%%%%%%%%%%
% Code creates one of two sample waveforms, performs zero crossing count,
% displays waveform and displays time between zero crossings
%%%%%%%%%%%%%%%%%%%%%%%%%%%%%%%%%%%%%%%%%%%%%%%%%%%%%%%%%%%%%%%%%%%%%%%%
%%%%%%%%%%%%%%%%%%%%%%%%%%%%%%%%%%%%%%%%%%%%%%%%%%%%%%%%%%%%%%%%%%%%%%%%
% author: Brad Christopher with assistance from Mathworks onramp training, online resources &
searches

clc
clear
% Parameters
fs = 80000; % Sampling rate in Hz
t = 0:1/fs:0.04; % Time vector for 1 second
A = 1;
% Generate the sine wave
% Sample waveform with Harmonics

x1 = A*sin(2*pi*48.75*t);
x2 = (0.5*A)*sin(2*pi*150*t);
x3 = (0.15*A)*sin(2*pi*250*t);
x4 = (0.5*A)*sin(2*pi*1042*t);
%xn = x1 + x2 + x3 + x4;
xn = x1 + x4;
% Count the zero crossings and get the intervals
[count, intervals] = count_Z_cross(xn, fs);
% Display the results
disp(['Number of zero crossings: ', num2str(count)]);
disp(['Time intervals between zero crossings (in seconds):']);
disp(intervals);
% Plot of waveform
plot(t, xn); %real(xn_filtered_interp)); %real - imag
xlim([0 0.04])
title('Zero Crossing Example');
xlabel('Time (s)');
ylabel('Amplitude');
grid on;

```

Function for zero crossing count

```

function [count, intervals] = count_Z_cross(signal, fs)
% Ensure the signal is a column vector
signal = signal(:);

% Calculate the zero crossings

```

```
zeroCrossings = find(diff(sign(signal)) ~= 0);
```

```
% Count the zero crossings
count = length(zeroCrossings);
```

```
% Calculate the time intervals between zero crossings
intervals = diff(zeroCrossings) / fs;
```

```
end
```

RoCoF SA Recreation

```
%%%%%%%%%%%%%%%%%%%%%%%%%%%%%%%%%%%%%%%%%%%%%%%%%%%%%%%%%%%%%%%%%%%%%%%%
%%%%%%%%%%%%%%%%%%%%%%%%%%%%%%%%%%%%%%%%%%%%%%%%%%%%%%%%%%%%%%%%%%%%%%%%
% Code creates one sample waveform with , performs zero crossing count,
% displays waveform and displays time between zero crossings
%%%%%%%%%%%%%%%%%%%%%%%%%%%%%%%%%%%%%%%%%%%%%%%%%%%%%%%%%%%%%%%%%%%%%%%%
%%%%%%%%%%%%%%%%%%%%%%%%%%%%%%%%%%%%%%%%%%%%%%%%%%%%%%%%%%%%%%%%%%%%%%%%
% author: Brad Christopher with assistance from Mathworks onramp training, online resources &
searches
clc
clear
%%% Plots for the limits of RoCoF %%%
t = 0:0.02:10; % time for plot 1/2 sec increments
% recreate south aust event 28-9-2016 16:18
time_stamp = [0 0.25 0.5 0.55 0.58 0.6 0.62 0.65 0.66 0.7 0.73 0.8 0.81 0.9 1 1.05 1.15 1.21 1.3
1.31 1.35 1.38 1.4 1.45 1.46 1.47 1.51 1.6 1.63 1.7 1.8];
freq_Value = [49.75 49.85 49.8 49.8 49.83 49.82 49.83 49.73 49.62 49.5 49.5 49.5 49.6 49.5 49.4
49.35 49.35 49.25 49.45 49.25 47.35 46.75 46.8 48.15 48.7 48.75 49.125 48.125 47.85 47.25
46.625 ];
interpol_val = interp1(time_stamp,freq_Value,t,'linear');
plot (t,interpol_val, 'LineWidth', 0.5, 'DisplayName', 'Interpolated Data');
xlabel('Time (seconds)');
ylabel('Frequency (Hz)');
title('Interpolation of South Australia Event Data');
grid on
% looking at the 1.3 seconds where the RoCof starts - trim the data for
% just this period - this is just to prove the rocof calcs based on a
% sample
data = [t', interpol_val']; % Time values and interpol freq's
trim_point = (t >= 1.3) & (t <= 1.8); % cuts off at 1.3 seconds
trim_data = data(trim_point,:); %trims data to suit trim time
display (trim_data);
rocof_time = trim_data(:,1); % seperates time data
rocof_freq = trim_data(:,2); % seperates freq data
% RoCoF calc
RoCoF = diff(rocof_freq)./ diff(rocof_time);
avg_rocof = mean(RoCoF); %averages rocof values
disp('RoCoF');
disp(avg_rocof);
```



Sliding Window DFT

```

%%%%%%%%%%%%%%%%%%%%%%%%%%%%%%%%%%%%%%%%%%%%%%%%%%%%%%%%%%%%%%%%%%%%%%%%
%%%%%%%%%%%%%%%%%%%%%%%%%%%%%%%%%%%%%%%%%%%%%%%%%%%%%%%%%%%%%%%%%%%%%%%%
% New code to demonstrate real time DFT. This code uses a fixed 50 hz clean
% signal. It generates its own random rocof excursions - deliberately set
% to exceed the operating standards. Any excursions are time stamped and an
% error message is generated for a sys operator
%%%%%%%%%%%%%%%%%%%%%%%%%%%%%%%%%%%%%%%%%%%%%%%%%%%%%%%%%%%%%%%%%%%%%%%%
%%%%%%%%%%%%%%%%%%%%%%%%%%%%%%%%%%%%%%%%%%%%%%%%%%%%%%%%%%%%%%%%%%%%%%%%
% author: Brad Christopher with assistance from Mathworks onramp training, online resources &
% searches

clc
clear
% settings
fs = 1000; % Sampling frequency (1000 samples per second)
t = 0:1/fs:10;% Time vector for 5 seconds of simulation
f = 50; % Initial frequency (50 Hz)
N = fs / f;% Samples per cycle for 50 Hz
rocof_span = 0.5;% RoCoF dip period min 0.5s
rocof_freq = rand(1, 5);% Random RoCoF/ random frequency changes 5 is an arbitrary amount
window_len = 0.5;% Sliding window length sec
window_size = fs * window_len; % Number of samples in the sliding DFT window
zero_padding_factor = 100;% Zero-padding
% Event capture threshold
threshold = 0.05;% ±0.5 Hz 50 Hz based on freq standards (char 177 - ±)
rocof_limit = 1;% Rocof threshold of ±1 Hz/s
% Randomize when RoCoF events occur during the 5 seconds
rocof_times = rand(1, 5) * (length(t) - fs * rocof_span); % Random rocof start times
rocof_times = round(rocof_times); % this brings start time back to whole integer values
% as some will possibly be decimal values
% Frequency variation over time
frequency = f * ones(size(t));
for i = 1:length(rocof_times)
    end_time = rocof_times(i) + rocof_span * fs;
    frequency(rocof_times(i):end_time) = f - rocof_freq(i); % subtracts the rand rocof ...
    % event from the 50 hz in the vector that aligns with the time
end
% Frequency signal with variations
signal = sin(2 * pi * cumsum(frequency) / fs); % cumulative sum the resultant waveform
% Sliding DFT monitoring every 10 ms
monitoring_interval = 0.01; % Monitoring every 10 ms
monitor_samples = round(monitoring_interval * fs); % ensuring interger value - so some rounding
is occurring
sliding_window = zeros(1, window_size); % Initialize sliding DFT window
frequencies_monitored = zeros(1, ceil(length(t) / monitor_samples)); % Store monitored
frequencies - Ceil rounds up to inetger value

```

```

time_monitored = zeros(1, length(frequencies_monitored)); % ensure each freq has associate time
recorded
% Matrix/s to store excursions and ROCOF events
excursion_times = [];
excursion_frequencies = [];
rocof_times = [];
rocof_values = [];
% Monitoring the frequency using a sliding DFT
count = 1;
for i = 1:monitor_samples:length(t)
    if i+window_size-1 > length(t)
        % If remaining samples are fewer than the window size, pad the remaining window with
        zeros
        sliding_window = [signal(i:end), zeros(1, window_size - length(signal(i:end)))];
    else
        sliding_window = signal(i:i+window_size-1); % Current window of the signal
    end

    % Zero-padding for improved frequency resolution
    padded_window_size = window_size * zero_padding_factor;
    Y = fft(sliding_window, padded_window_size); % Perform FFT on the zero-padded window

    % Find the peak frequency in the magnitude spectrum
    [~, max_idx] = max(abs(Y(1:padded_window_size/2))); % Find the peak in the first half
    estimated_freq = (max_idx - 1) * fs / padded_window_size; % Estimate the frequency

    frequencies_monitored(count) = estimated_freq; % Store the results
    time_monitored(count) = t(i);

    % Event capture: Check for frequency excursions beyond  $\pm 0.5$  Hz from 50 Hz
    if abs(estimated_freq - 50) > threshold
        excursion_frequencies = [excursion_frequencies, estimated_freq];
        excursion_times = [excursion_times, t(i)];
    end
    % issues with pre-allocation for above - not sure - time permitting
    % will return to it.
    % ROCOF detection: Check rate of change of frequency over 500 ms (50 samples)
    if count > 50
        freq_change = estimated_freq - frequencies_monitored(count - 50); % 500 ms prior
        rocof = freq_change / 0.5; % ROCOF in Hz/sec (change per 500 ms)

        % Check if ROCOF exceeds threshold
        if abs(rocof) > rocof_limit
            rocof_times = [rocof_times, t(i)]; % same pre allocate issues here
            rocof_values = [rocof_values, rocof];
            fprintf('ROCOF event detected at %.2f seconds with ROCOF = %.2f Hz/s\n', t(i), rocof);
        end
    end

    count = count + 1;
end
% Plot the results
figure;
subplot(3,1,1);
plot(t, frequency, 'b', 'LineWidth', 1.5);
title('Original Frequency with Random RoCoF Dips');

```




```
xlabel('Time (s)');  
ylabel('Frequency (Hz)');  
grid on;  
subplot(3,1,2);  
plot(time_monitored(1:count-1), frequencies_monitored(1:count-1), 'r', 'LineWidth', 1.5); % count-1  
title('Sliding DFT Estimated Frequency');  
xlabel('Time (s)');  
ylabel('Frequency (Hz)');  
xlim([0 9.5]);  
grid on;
```